atmosphere

MDPI

Article

Model Inter-Comparison for $PM_{2.5}$ Components over urban Areas in Japan in the J-STREAM Framework

Kazuyo Yamaji [1,*], Satoru Chatani [2], Syuichi Itahashi [3], Masahiko Saito [4], Masayuki Takigawa [5], Tazuko Morikawa [6], Isao Kanda [7], Yukako Miya [8], Hiroaki Komatsu [9], Tatsuya Sakurai [10], Yu Morino [2], Kyo Kitayama [2], Tatsuya Nagashima [2], Hikari Shimadera [11], Katsushige Uranishi [11], Yuzuru Fujiwara [12], Tomoaki Hashimoto [12], Kengo Sudo [13], Takeshi Misaki [1,14] and Hiroshi Hayami [3]

1 Graduate School of Maritime Sciences, Kobe University, Kobe, Hyogo 658-0022, Japan; misaki@tepsco.co.jp
2 National Institute for Environmental Studies, Tsukuba, Ibaraki 305-8506, Japan; chatani.satoru@nies.go.jp (S.C.); morino.yu@nies.go.jp (Y.M.); kitayama.kyo@nies.go.jp (K.K.); nagashima.tatsuya@nies.go.jp (T.N.)
3 Central Research Institute of Electric Power Industry, Abiko, Chiba 270-1194, Japan; isyuichi@criepi.denken.or.jp (S.I.); haya@criepi.denken.or.jp (H.H.)
4 Ehime University, Matsuyama, Ehime 790-8566, Japan; msaito@agr.ehime-u.ac.jp
5 Japan Agency for Marine—Earth Science and Technology, Yokohama, Kanagawa 236-0001, Japan; takigawa@jamstec.go.jp
6 Japan Automobile Research Institute, Tsukuba, Ibaraki 305-0822, Japan; tmorikaw@jari.or.jp
7 Japan Meteorological Corporation, Osaka 556-0021, Japan; isao.kanda@n-kishou.co.jp
8 Japan Weather Association, Toshima, Tokyo 170-6055, Japan; yukako@jwa.or.jp
9 Kanagawa Environmental Research Center, Hiratsuka, Kanagawa 254-0014, Japan; komatsu.amti@pref.kanagawa.jp
10 School of Science and Engineering, Meisei University, Hino, Tokyo 191-8506, Japan; tatsuya.sakurai@meisei-u.ac.jp
11 Graduate School of Engineering, Osaka University, Suita, Osaka 565-0871, Japan; shimadera@see.eng.osaka-u.ac.jp (H.S.); k.uranishi2@gmail.com (K.U.)
12 Suuri-Keikaku, Chiyoda, Tokyo 101-0003, Japan; fujiwara@sur.co.jp (Y.F.); hashimoto_tomoaki@sur.co.jp (T.H.)
13 Graduate School of Environmental Studies, Nagoya University, Nagoya, Aichi 464-8601, Japan; kengo@nagoya-u.jp
14 Tokyo Electric Power Services Co., Ltd., Koto, Tokyo 135-0062, Japan
* Correspondence: kazuyo@maritime.kobe-u.ac.jp; Tel.: +81-78-431-6282

Received: 14 January 2020; Accepted: 19 February 2020; Published: 25 February 2020

Abstract: A model inter-comparison of secondary pollutant simulations over urban areas in Japan, the first phase of Japan's study for reference air quality modeling (J-STREAM Phase I), was conducted using 32 model settings. Simulated hourly concentrations of nitric oxide (NO) and nitrogen dioxide (NO_2), which are primary pollutant precursors of particulate matter with a diameter of 2.5 μm or less ($PM_{2.5}$), showed good agreement with the observed concentrations, but most of the simulated hourly sulfur oxide (SO_2) concentrations were much higher than the observations. Simulated concentrations of $PM_{2.5}$ and its components were compared to daily observed concentrations by using the filter pack method at selected ambient air pollution monitoring stations (AAPMSs) for each season. In general, most models showed good agreement with the observed total $PM_{2.5}$ mass concentration levels in each season and provided goal or criteria levels of model ensemble statistics in warmer seasons. The good performances of these models were associated with the simulated reproducibility of some dominant components, sulfates (SO_4^{2-}) and ammonium (NH_4^+). The other simulated $PM_{2.5}$ components, i.e., nitrates (NO_3^-), elemental carbon (EC), and organic carbon (OC), often show clear deviations from the observations. The considerable underestimations (approximately 30 μg/m^3 for total $PM_{2.5}$) of all participant models found on heavily polluted days with approximately 40–50 μg/m^3 for total

$PM_{2.5}$ indicated some problems in the simulated local meteorology such as the atmospheric stability. This model inter-comparison suggests that these deviations may be owing to a need for further improvements both in the emission inventories and additional formation pathways in chemical transport models, and meteorological conditions also require improvement to simulate elevated atmospheric pollutants. Additional accumulated observations are likely needed to further evaluate the simulated concentrations and improve the model performance.

Keywords: $PM_{2.5}$; $PM_{2.5}$ components; three-dimensional chemical transport model; model inter-comparison; urban scale; secondary particles

1. Introduction

Particulate matter (PM) consists of a complex mixture of solid and liquid particles of organic and inorganic substances suspended in the atmosphere. The major components of PM are sulfates (SO_4^{2-}), nitrates (NO_3^-), ammonium (NH_4^+), sodium chloride (NaCl), black carbon (BC) or elemental carbon (EC), organic carbon (OC), mineral dust, and water. The PMs with the greatest negative health effects are those with a diameter of 2.5 μm or less ($PM_{2.5}$), which can penetrate and lodge deep inside the lungs [1]. Some PMs are also climate-dependent, known as short-lived climate pollutants (SCLPs) [2]. Warming due to sunlight absorption (e.g., BC) and cooling due to sunlight scattering (e.g., SO_4^{2-}) directly affect radiative forcing in the earth's climate system. Additionally, water-soluble PMs affect the regional climate system interacting with cloud microphysics. These radiative and microphysical interactions can induce changes in regional precipitation and atmospheric circulation patterns. Some $PM_{2.5}$ particles are directly emitted from natural sources and human activities, while others are formed through complex oxidation reactions and particle agglomeration. Combining the regional three-dimensional chemical transport model (CTM) with comprehensive particulate formations may be a useful tool for understanding the detailed behavior of short-lived $PM_{2.5}$ components in the atmosphere.

Recently, $PM_{2.5}$ air quality has been improved in East Asian countries, e.g., China [3] and Japan [4]; however, $PM_{2.5}$ concentrations at Japanese air pollution monitoring stations (APMSs) have not met yet the environmental quality standard, defined as 15 μg/m^3 for the annual $PM_{2.5}$ mean and 35 μg/m^3 for 24-h $PM_{2.5}$ mean, or the World Health Organization (WHO) air quality guidelines, with corresponding values of 10 and 35 μg/m^3. An established reference regional CTM system should be applied to design effective $PM_{2.5}$ control strategies [5]. However, accurately reproducing or predicting the concentrations and distributions of $PM_{2.5}$ and its relevant substances remains challenging, due to inaccurate emission inventories, poorly represented initial and boundary conditions, imperfect physical, dynamical, and chemical parameterizations, and limited observations for verification, as noted for previous Asian scale model inter-comparisons, i.e., the model inter-comparison study for Asia (MICS-Asia) series [6–9] and the urban air quality model inter-comparison study in Japan (UMICS) series [10–12].

A model inter-comparison framework, Japan's study for reference air quality modeling (J-STREAM), was designed to establish a reference regional CTM system to consider strategies for reducing $PM_{2.5}$ and its relevant substances [5]. In this paper, the capacities of participant models for J-STREAM to simulate $PM_{2.5}$ and its components were evaluated for two urban areas in Japan in each season. The model improvements will be discussed based on the inter-model differences.

2. Methodology

2.1. Framework of J-STREAM Phase I

A model inter-comparison project in Japan, J-STREAM, was initiated in 2016. One aim of J-STREAM is to investigate differences in simulated concentrations of secondary atmospheric pollutants such as $PM_{2.5}$ components and ozone over urban areas in Japan due to differences between model frames and/or

model settings, including boundary and inputted conditions and physical and chemical mechanisms. Detailed model settings are described below. Furthermore, these including an introduction of J-STREAM can be found in previous research for the overview [5] and the performance on ozone [13].

The main target of the first phase of J-STREAM (J-STREAM Phase I) is to evaluate the general performances of participant models on secondary atmospheric concentrations over urban areas in Japan. Daily concentrations of $PM_{2.5}$ components in each season among others were treated as subjects of evaluation in this paper. The enhanced simulation periods of J-STREAM Phase I were the spring of 2013, 27 April–26 May 2013, the summer of 2013, 12 July–10 August 2013, the autumn of 2013, 11 October–9 November 2013, and the winter of 2014, 10 January–8 February 2014, which corresponded to the seasonal periods of the national observation frame for $PM_{2.5}$ components (Table 1). The detailed evaluations and additional experiments for individual participant models can be found in [14].

Table 1. Dates of enhanced simulation periods for model evaluations including a simulation spin-up. Updated from the overview of Japan's study for reference air quality modeling (J-STREAM) [5].

Season	Dates
Spring 2013	27 April–26 May 2013
Summer 2013	12 July–10 August 2013
Autumn 2013	11 October–9 November 2013
Winter 2014	10 January–8 February 2014

Four nested model domains, d01, d02, d03, and d04, on a Lambert conformal map projection were employed in the J-STREAM project [5]. The finest domains, d03 and d04, with a 5 × 5 km grid, cover the major city clusters in western Japan, including Osaka, Kobe, Kyoto, and Nagoya, and the Tokyo metropolitan area, respectively. Simulated concentrations in the d03 and d04 domains were used for model evaluations, and the results are discussed in following sections. Figure 1 shows the d03 and d04 domains, including the locations of ambient APMSs (AAPMSs), for which simulated concentrations were evaluated via comparisons with observations.

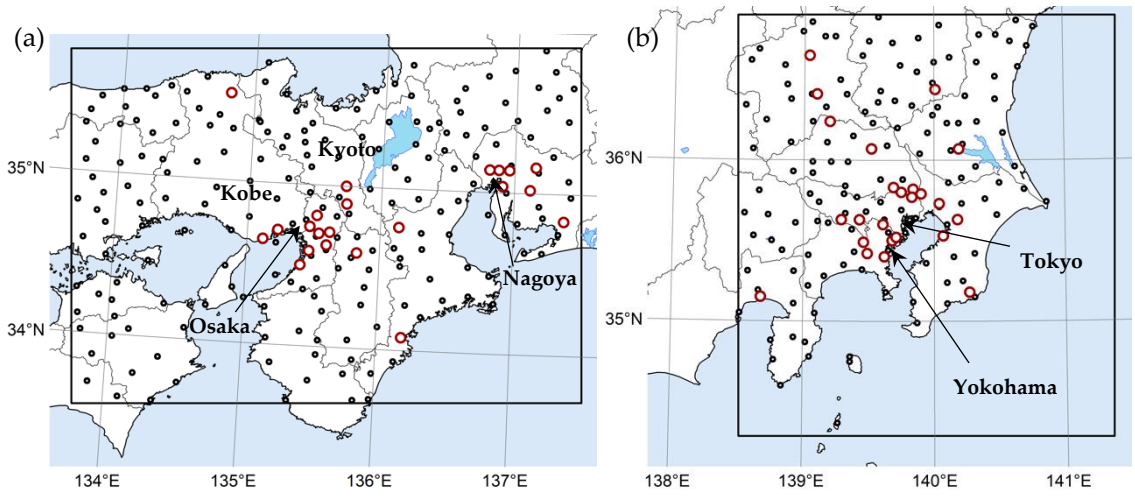

Figure 1. Finest model domains for J-STREAM, d03 (**a**) and d04 (**b**). d03 covers major city clusters located in western Japan including Osaka, Kobe, Kyoto, and Nagoya. d04 covers the Tokyo metropolitan area. The red circles indicate the locations of ambient air pollution monitoring stations (AAPMSs). The black circles indicate the locations of the meteorological observation stations of the Japan Meteorological Agency (JMA).

2.2. Baseline Meteorological Model Configurations

The baseline meteorological simulation for J-STREAM Phase I was performed by the Weather Research and Forecasting (WRF) model, using the Advanced Research WRF (ARW) Version 3.7.1 [15]. The WRF inputted data were acquired from the National Centers for Environmental Prediction Final Operational Model Global Tropospheric Analyses (ds083.2) with a 1 × 1 degree resolution [16] and the Real-Time, Global Sea Surface Temperature High-Resolution (RTG_SST_HR) analysis with a 1/12 × 1/12 degree resolution [17] and a temporal resolution of 6 h for the initial and boundary conditions. The horizontal configurations of the one-way nested model domains, d01, d02, d03, and d04, are 220 × 170 grids with a 45-km horizontal resolution, 154 × 160 grids with a 15-km resolution, 82 × 61 grids with a 5-km resolution, and 64 × 70 grids with a 5-km resolution, respectively. The vertical grid structure consists of 31 layers from the surface to the model top (100 hPa). Five grids were trimmed off each of the four lateral boundaries for the offline CTMs. The physics parameterizations applied in this model included the WRF Single-Moment 5-class scheme [18], the Radiative Transfer Model (RRTM) [19] for a longwave radiation scheme, the Dudhia scheme [20] for a shortwave radiation scheme, the Noah Land Surface Model [21], the Mellor-Yamada Nakanishi and Niino surface layer scheme level 2.5 [22], and the Kain-Fritsch convective parameterization [23] for d01 and d02. No convection parameterization was used for the 5-km domains. The grid-nudging four-dimensional data assimilation technique was employed for wind, temperature, and water vapor from level 11 (approximately 2 km) to the top of the model at 100 hPa with the nudging coefficients of 1.0×10^{-4} and 0.5×10^{-5} s^{-1} for d01 and d02, respectively. Most of the participant CTMs employed baseline meteorological fields, while others employed the meteorology based on different model settings. The differences in the model settings in some participant models are described in Section 2.3.

The baseline meteorological fields were compared with hourly observations of the Japan Meteorological Agency (JMA) for the observation stations within d03 and d04 (Figure 1) over four seasons: the spring of 2013 (11–26 May 2013), the summer of 2013 (27 July–10 August 2013), the autumn of 2013 (25 October–9 November 2013), and the winter of 2014 (24 January–7 February 2014) (Figures 2 and 3). The hourly observed and modeled meteorological variables were averaged for all meteorological observatories for each domain.

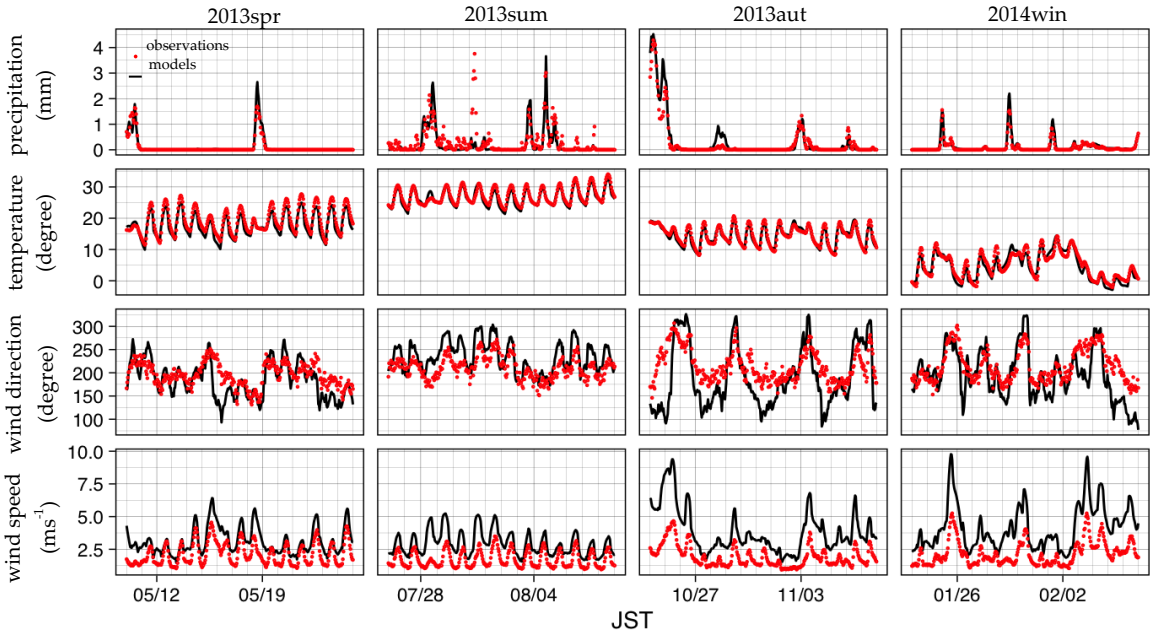

Figure 2. Spatially averaged precipitation, temperature, wind direction, and wind speed over four seasons. These results are based on hourly observed values and simulated at all JMA stations for d03.

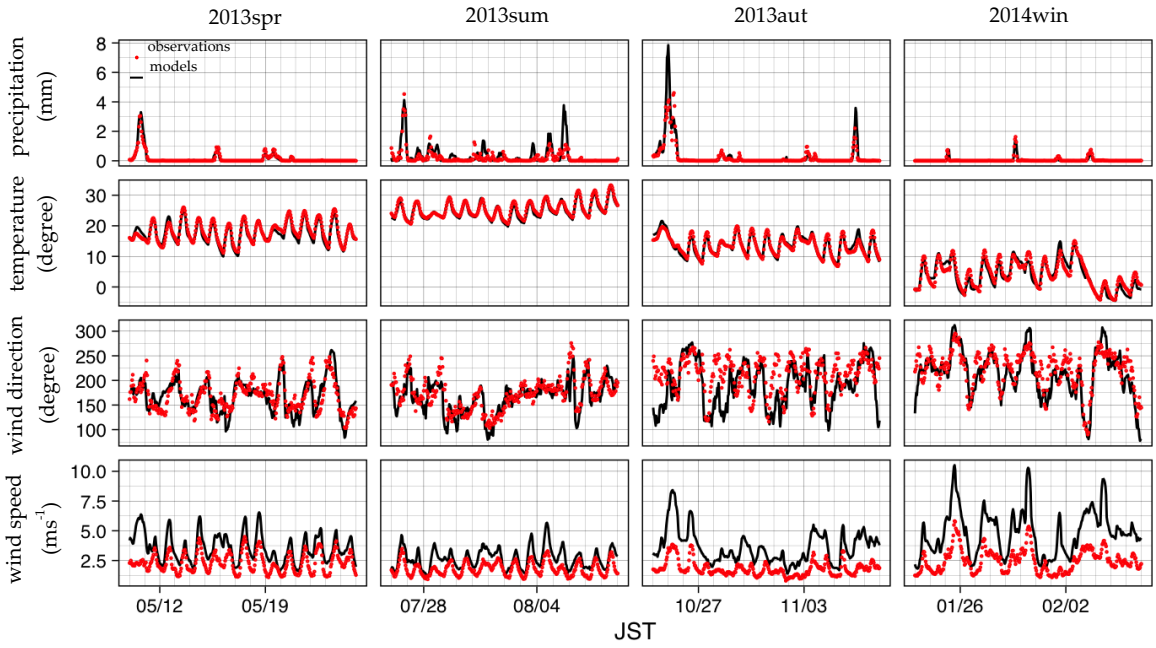

Figure 3. Spatially averaged precipitation, temperature, wind direction, and wind speed over the four seasons. These results are based on hourly observed values and simulated at all JMA stations for d04.

The WRF using the baseline setting can generally simulate the observed meteorological conditions well. Meanwhile, WRF tended to overestimate the observed wind speeds. This was likely affected by the sparse horizontal resolution and coarse land information. The simulation performance of wind patterns was slightly better for d04 than that for d03 (Figures 2 and 3). However, simulated precipitation timing and their amounts were consistent with the observations (Figures 2 and 3).

2.3. Chemical Transport Model Configurations

A total of 32 simulations were performed using three types of regional CTMs in J-STREAM Phase I: Community Multiscale Air Quality (CMAQ) [24], Comprehensive Air quality Model with eXtensions (CAMx) [25], and Weather Research and Forecasting-Chemistry (WRF-Chem) [26]. Table 2 presents the configurations of the employed models. All participants conducted J-STREAM simulation under their own usual simulation conditions. The CMAQ group (M01–M28) included several versions, i.e., chemical mechanisms: Statewide Air Pollution Research Center mechanism (SAPRC) 99 [27], SAPRC07 [28], Carbon Bond (CB) 05 [29], and Regional Atmospheric Chemistry Mechanism (RACM) 2 [30], and three types of CMAQ aerosol calculation techniques [31]: aero5, aero6, and aero6 with the volatility basis set (VBS) approach [32]. These CMAQ aerosol calculation techniques employed ISORROPIA Version 1 [33,34] as an aerosol thermodynamic model and the second version of ISORROPIA (ISORROPIA Version 2) for updating the crustal species thermodynamics, the speciation schemes, and the SO_4^{2-} formation pathway [35] for versions after 5.0. The basic techniques of aero5 and aero6 include secondary organic aerosol (SOA) formation processes based on empirical parameters for SOA yields [36]. Major or minor updates were reflected in the chemical and aerosol mechanisms in the later versions. One CAMx model (M29) applied in J-STREAM used the SAPRC07 chemistry and the coarse and fine aerosol scheme treating both static coarse and fine mode aerosols [37]. The WRF-Chem group (M30–M32) included two Versions (3.8.1 and 3.7.1) that employed RADM2: the aerosol module of the Modal Aerosol Dynamics Model for Europe (MADE) [38] and the SOA Model (SORGAM) [39].

As described in detail in an overview article on J-STREAM [5], participants were requested to run CTM simulations during the enhanced target periods of four seasons for d03 or d04. As shown in Table 2, the simulations for some participant models began at d01 (M02, M03, M07–M15, M20, and M30–M32), but others began from the more inner domains. Fifteen participant models (M01–07, M14,

M15, M21–M24, M26, M29, and M30) submitted their results for both domains for all four seasons, but the other participants submitted results for only selected seasons, with the highest number of model results for the summer of 2013.

Initial concentrations on the first day of each season and boundary concentrations throughout the entire target period were generated in the simulation using the M15 setting via CMAQ Version 5.0.2 with the SAPRC07–aero6 mechanisms for d01 and d02. Boundary concentrations for d01 of M15 were obtained from results for a chemical atmospheric general circulation model designed for studying atmospheric environment and radiative forcing, CHASER [40] for the Hemispheric Transport of Air Pollution (HTAP) Version 2 [41]. In J-STREAM Phase I, model-ready mosaic emission data corresponding to all participant chemical–aerosol mechanisms involving multiple emission inventories and results from an emission model for biogenic volatile organic compounds were provided: HTAP Version 2.2 [42] and Global Fire Emissions Database Version 4.1 [43] for Asian anthropogenic emissions, the Japan Auto–Oil Program (JATOP) emission inventory database (JEI-DB) [44], the updated JEI–DB [5], and Sasakawa Peace Foundation emissions for ships for Japanese anthropogenic emissions, volcanic emission data from Aerosol Comparisons between Observations and Models (AeroCom) [45] and JMA [46], and estimations obtained by using Model of Emissions of Gases and Aerosols from Nature Version 2.1 [47]. Most participant CTMs used model-ready input data; however, some participant CTMs performed simulations in their own emission frames. M03 used EAGrid2010-JAPAN [48], and M20 and M27 used EAGrid2000-JAPAN [49] for anthropogenic emissions in Japan. For the Asian scale anthropogenic emissions, M20 employed NASA INTEX-B [50] instead of HTAP Version 2.2. Additionally, some CTMs employed different emission injection heights. The Model for Ozone and Related chemical Tracers Version 4 (MOZART-4) [51], for instance, was used as boundary conditions in some model settings.

As mentioned in Section 2.2., most of the participants employed the baseline meteorological fields; however, other CTMs (M07, M20) used WRF-ARW outputs based on their own conditions, including physical options, parameterizations, and a fine input meteorological analysis data, which is the grid point value derived from the mesoscale model (GPV MSM) data by JMA.

Table 2. Configurations of participant chemical transport models (CTMs) submitted for J-STREAM Phase I, updated from an overview of J-STREAM [5].

ID	Model	Version	Chemical Mechanism	Aerosol Module	Photolysis	Simulation [1]				Emis [2]	BCON [3]	Met [4]	Submitted [5]	
						d01	d02	d03	d04				d03	d04
M01	CMAQ	5.2	CB05	aero6	inline			o	o	o	o	o	o	o
M02	CMAQ	5.1	SAPRC07	aero6	inline	o	o	o	o	o	o	o	o	o
M03	CMAQ	5.1	SAPRC07	aero6	inline	o	o	o	o	E1	o	o	o	o
M04	CMAQ	5.1	SAPRC07	aero6	inline			o	o	o	o	o	o	o
M05	CMAQ	5.1	SAPRC07	aero6	inline			o	o	o	o	o	o	o
M06	CMAQ	5.1	SAPRC07	aero6	table			o	o	o	o	o	o	o
M07	CMAQ	5.0.2	SAPRC07	aero6	inline	o	o	o	o	o	M	W	o	o
M08	CMAQ	5.0.2	SAPRC07	aero6	inline	o	o	o	o	o	o	o	o	o
M09	CMAQ	5.0.2	CB05	aero6	inline	o	o	o	o	o	o	o	o	o
M10	CMAQ	5.0.2	CB05	aero6	inline	o	o	o	o	o	o	o	su	su
M11	CMAQ	5.0.2	CB05	aero6vbs	inline	o	o	o	o	o	o	o	su	su
M12	CMAQ	5.0.2	RACM2	aero6	inline	o	o	o	o	o	o	o	o	o
M13	CMAQ	5.0.2	SAPRC99	aero5	inline	o	o	o	o	o	o	o	o	o
M14	CMAQ	5.0.2	SAPRC07	aero6	inline	o	o	o	o	o	o	o	o	o
M15	CMAQ	5.0.2	SAPRC07	aero6	inline	o	o	o	o	o	o	o	o	o
M16	CMAQ	5.0.2	SAPRC07	aero6	inline			o	o	o	o	o	su	su
M17	CMAQ	5.0.2	CB05	aero6	inline			o	o	o	o	o	su	su
M18	CMAQ	5.0.2	RACM2	aero6	inline			o	o	o	o	o	su	su
M19	CMAQ	5.0.2	SAPRC99	aero5	inline			o	o	o	o	o	su	su
M20	CMAQ	5.0.1	SAPRC99	aero5	inline	o	o	o		E2	D	W	o	
M21	CMAQ	5.0.1	SAPRC07	aero6	inline	o		o	o	o	o	o	o	o
M22	CMAQ	5.0.1	SAPRC07	aero6	inline			o	o	o	o	o	o	o
M23	CMAQ	5.0.1	SAPRC07	aero6	inline			o	o	o	o	o	o	o
M24	CMAQ	5.0.1	CB05	aero6	inline			o	o	o	o	o	o	o

Table 2. *Cont.*

ID	Model	Version	Chemical Mechanism	Aerosol Module	Photolysis	Simulation [1]				Emis [2]	BCON [3]	Met [4]	Submitted [5]	
						d01	d02	d03	d04				d03	d04
M25	CMAQ	5.0.1	SAPRC99	aero5	inline				o	o	o	o		o
M26	CMAQ	5.0.1	SAPRC99	aero5	inline			o	o	o	o	o	o	o
M27	CMAQ	4.7.1	SAPRC99	aero5	table				o	E3	o	o		o
M28	CMAQ	4.7.1	SAPRC99	aero5	table				o	o	o	o		o
M29	CAMx	6.4	SAPRC07	CF	table			o	o	o	o	o	o	o
M30 [6]	WRF-Chem	3.7.1	RADM2	MADE	inline	o	o	o	o	o	M	WC	o	o
M31	WRF-Chem	3.7.1	RADM2	MADE	inline	o	o	o	o	o	M	WC	su	su
M32	WRF-Chem	3.7.1	RADM2	MADE	inline	o	o	o	o	o	M	WC	su	su

[1] "o" indicates the domains that participants used to conduct their simulations. [2] Input emissions. "o" indicates that the baseline model-ready emission is used. "E1" uses EAGrid2010-JAPAN [48] and HTAP Version 2.2 [42]. "E2" uses EAGrid2000-JAPAN [49] and NASA INTEX-B [50]. "E3" uses EAGrid2000-JAPAN [49]. [3] Boundary concentration. "o" indicates that the baseline boundary concentration is used. "M" uses MOZART-4 [51]. "D" uses CMAQ defaults. [4] Meteorological condition. "o" indicates that the baseline metrological condition is used. "W" uses the meteorology simulated using WRF-ARW with own conditions, including physical options, parameterizations, and meteorological reanalysis. "WC" indicates the meteorology simulated using WRF-Chem with own conditions including physical options and parameterizations. [5] "o" indicates data submitted for d03 and d04 in each season. "su" was submitted for only summer. [6] NH_4^+ and total $PM_{2.5}$ were not submitted.

3. Observational Data for Model Evaluation

A monitoring framework of ambient $PM_{2.5}$ components was initiated in the fiscal year 2011 under the Japan government initiative [4]. Over a period of at least two weeks set for each season, 1-day accumulated concentrations of $PM_{2.5}$ components, including ions (e.g., SO_4^{2-}, NO_3^-, and NH_4^+), inorganic elements (e.g., Na, Al, K, and Ca), and carbonaceous aerosols (EC and OC), were monitored using the filter pack method at selected stations from three types of APMSs, including AAPMSs, roadside APMSs (RAPMSs), and background monitoring stations (BGMSs). $PM_{2.5}$ mass concentrations determined gravimetrically by weighing the filters were employed as the $PM_{2.5}$ mass concentration in this paper. Monitoring data from valid AAPMSs that obtained data for each $PM_{2.5}$ component over a period of at least eight days (53%) from each target period (up to 15 days) per each station were used to evaluate the performances of the participant CTMs. The number of valid AAPMSs was 16–22 stations for each domain and season. The data acquisition rate was highest in the summer, while a poor data acquisition rate was found for NO_3^- in autumn. Observed gaseous pollutants at these AAPMSs were also used to evaluate the simulated nitric oxide (NO), nitrogen dioxide (NO_2), and sulfur dioxide (SO_2).

Figures 4 and 5 present observed daily concentrations for $PM_{2.5}$ components, i.e., SO_4^{2-}, NO_3^-, NH_4^+, EC, and OC, and total $PM_{2.5}$ mass for each 12- to 15-day seasonal period at the AAPMSs for d03 and d04, respectively. The box-and-whisker and black dots (outliers) means the differences between AAPMSs in each domain.

In general, the concentrations of the total $PM_{2.5}$ and its components within a single domain exhibit similar day-to-day variabilities for each season. However, the frequency distributions of daily concentrations between the AAPMSs in each domain were enhanced, particularly for elevated concentrations (Figures 4 and 5). Therefore, the spatially averaged concentrations obtained from daily monitoring data for different AAPMSs within each domain were used for time series analysis hereafter.

For d03, i.e., western Japan, the seasonal-average total $PM_{2.5}$ concentrations were 17.3, 23.1, 20.3, and 19.6 μg/m^3, with maximum daily concentrations of 31.9, 37.6, 36.3, and 34.3 μg/m^3 for spring, summer, autumn, and winter. The summer $PM_{2.5}$ concentration was slightly higher than those for the other seasons; however, the seasonal characteristics of the $PM_{2.5}$ concentration are unclear. SO_4^{2-} was a dominant $PM_{2.5}$ component, accounting for approximately 40% (9.1 μg/m^3) of the total $PM_{2.5}$ mass concentration in the summer. Meanwhile, from autumn to winter, the ratios of $NO_3^-$and OC to total $PM_{2.5}$ mass increased. The ratios of the five major $PM_{2.5}$ components were similar, with values of 12%–19% in the winter. On the dates when $PM_{2.5}$ was elevated, the AAPMS differences in $PM_{2.5}$ concentration levels increased, and considerably high $PM_{2.5}$ was found at AAPMSs placed at major cities: Osaka and Nagoya. These results were compared with those from rural areas.

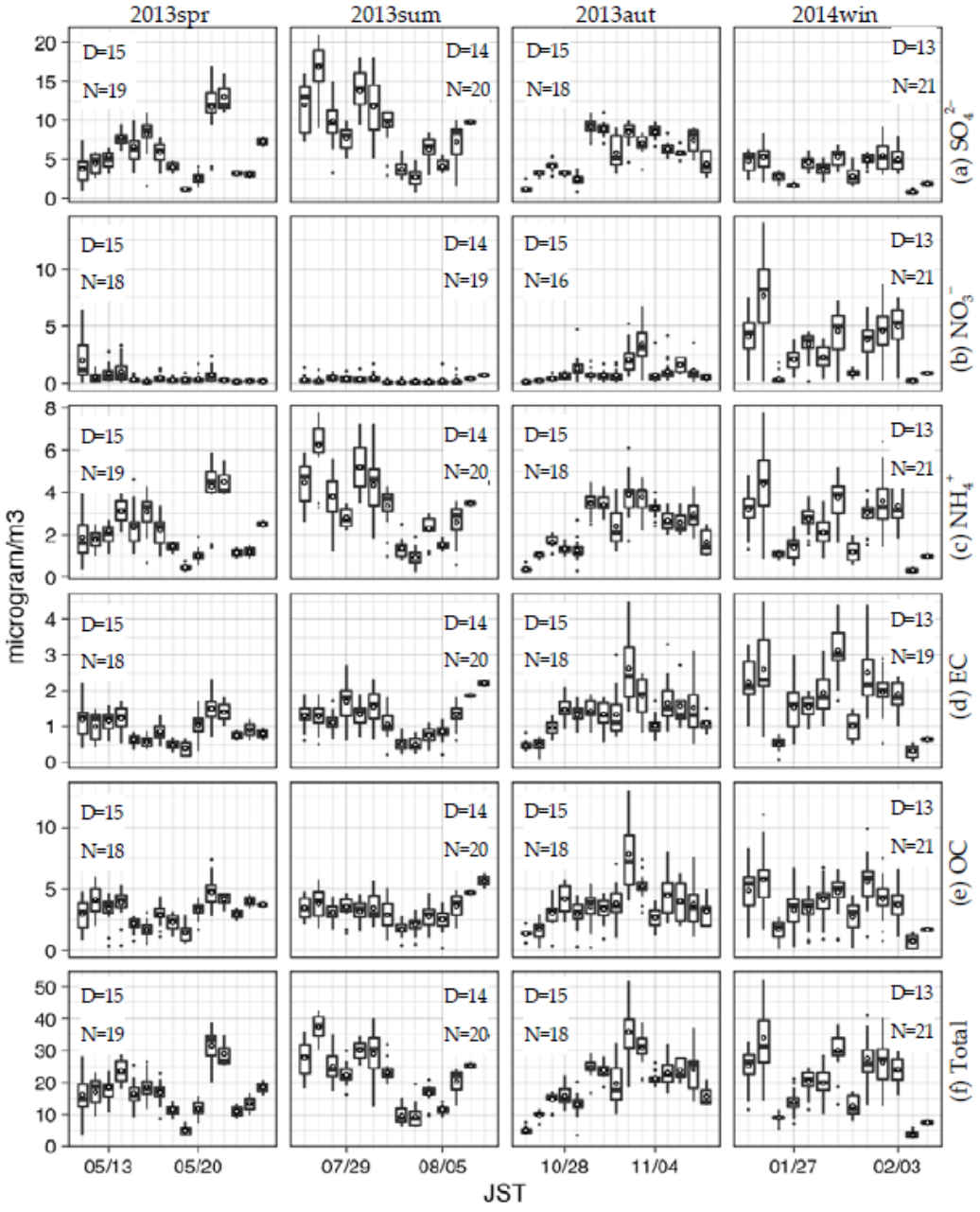

Figure 4. Box-plots of observed daily concentrations of total particulate matter with a diameter of 2.5 μm or less ($PM_{2.5}$) and its components: (**a**) sulfates (SO_4^{2-}), (**b**) nitrates (NO_3^-), (**c**) ammonium (NH_4^+), (**d**) elemental carbon (EC), (**e**) organic carbon (OC), and (**f**) total $PM_{2.5}$ mass, at AAPMSs within d03 for the four seasons. The open circles indicate spatially averages obtained from daily concentrations observed at AAPMSs within d03. The black dots indicate the outliers. The box-and-whisker and outliers represent the frequency distributions of daily concentrations observed at AAPMSs in d03. D presents the numbers of days with available observations, and N presents the number of AAPMSs.

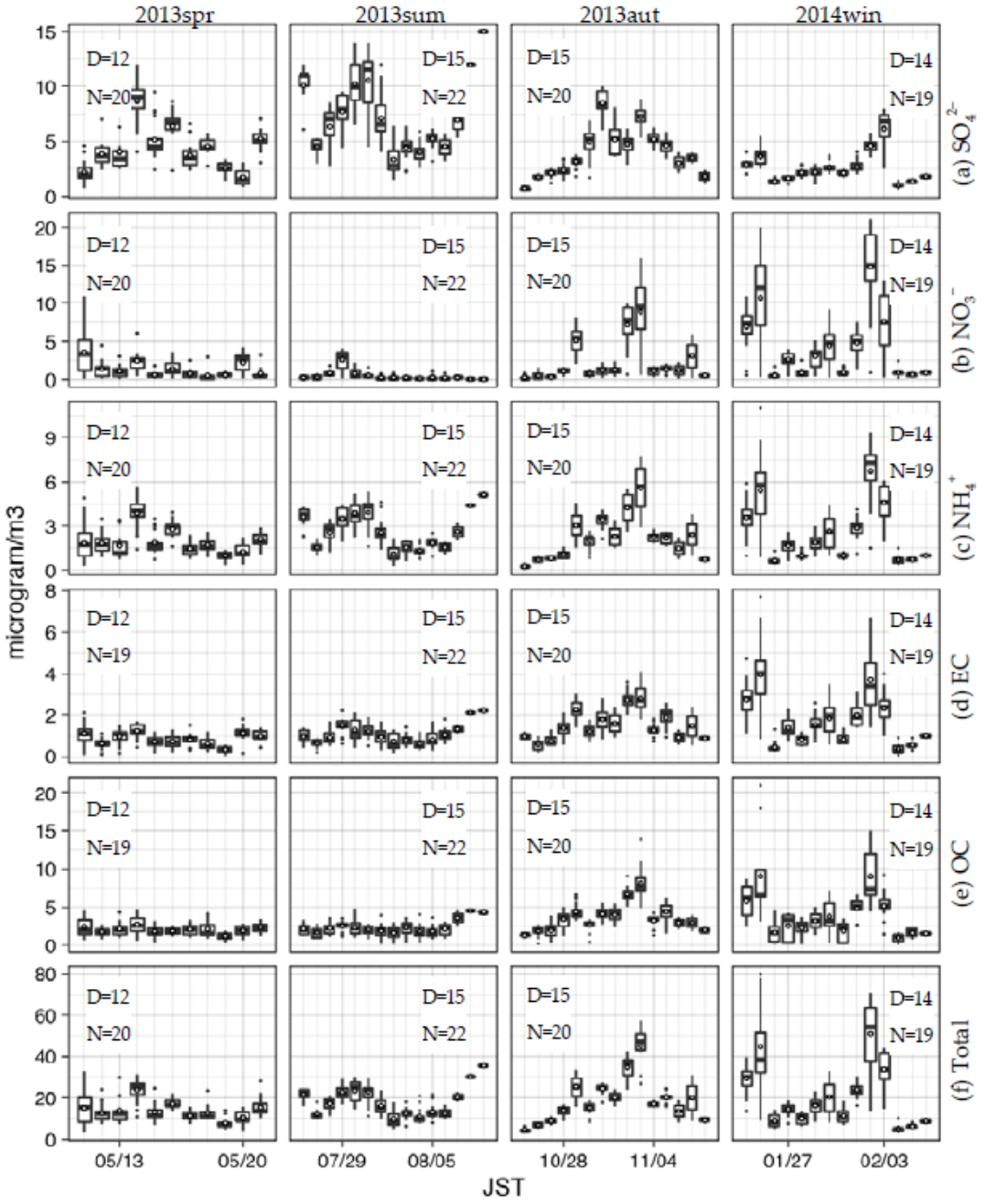

Figure 5. Box-plots of observed daily concentrations of total $PM_{2.5}$ and its components: (**a**) SO_4^{2-}, (**b**) NO_3^-, (**c**) NH_4^+, (**d**) EC, (**e**) OC, and (**f**) total $PM_{2.5}$ mass, at AAPMSs within d04 for the four seasons. The open circles indicate spatially averages obtained from daily concentrations observed at AAPMSs within d04. The black dots indicate the outliers. The box-and-whisker and outliers represent the frequency distributions of daily concentrations observed at AAPMSs in d04. D presents the numbers of days with available observations, and N presents the number of AAPMSs.

For d04, the Tokyo metropolitan area, which is several hundred kilometers east of d03, the day-to-day changes in the concentrations of total $PM_{2.5}$ and its components were similar to those for d03; however, the seasonal-average concentrations: 15.2, 18.6, 17.9, and 19.3 μg/m^3 for spring, summer, autumn, and winter, were slightly lower than those for d03; whereas the maximum daily concentrations were 26.3, 35.4, 41.9, and 46.8 μg/m^3. The elevated daily concentrations were obviously higher than those for d03 in the autumn and winter. Wintertime $PM_{2.5}$ concentrations were slightly

higher than those in the other seasons, with increased daily concentrations; however, the seasonal characteristics of the $PM_{2.5}$ concentration were unclear for d04. The daily variabilities of the total $PM_{2.5}$ mass were characterized by SO_4^{2-} in spring and summer, where the ratios of SO_4^{2-} to total $PM_{2.5}$ mass were 32% (4.8 μg/m^3) and 39% (4.8 μg/m^3), respectively. In autumn, the ratios of the other $PM_{2.5}$ components, including OC, NO_3^-, and NH_4^+, to the total $PM_{2.5}$ mass increased. The OC and NO_3^-concentrations were both higher than the SO_4^{2-} concentration in winter. In particular, for the first pollutant peak on 25 January, OC and NO_3^- were dominant, accounting for 22% (9.2 μg/m^3) and 23% (9.6 μg/m^3) of the total $PM_{2.5}$ mass concentration, respectively. For the peak on 2 February, NO_3^- was dominant, accounting for 22% (9.2 μg/m^3). SO_4^{2-} was the dominant $PM_{2.5}$ component throughout the year for d03, but for d04, OC and NO_3^- levels were higher than SO_4^{2-} levels in the winter. On the dates $PM_{2.5}$ elevated, the AAPMSs differences of $PM_{2.5}$ concentration levels were increased, and the considerably high $PM_{2.5}$ were found at the AAPMSs placed on the central area of d04, i.e., the Tokyo metropolitan area.

4. Results and Discussion

4.1. Hourly Concentrations of Primary Pollutants

Major gaseous pollutants were also monitored at the AAPMSs. Figures 6 and 7 present the spatial averages of observed and simulated hourly concentrations of NO, NO_2, and SO_2 from different AAPMSs for d03 and d04, respectively. Table 3 summarizes the ensemble performances of the participant CTMs at each AAPMS for each season.

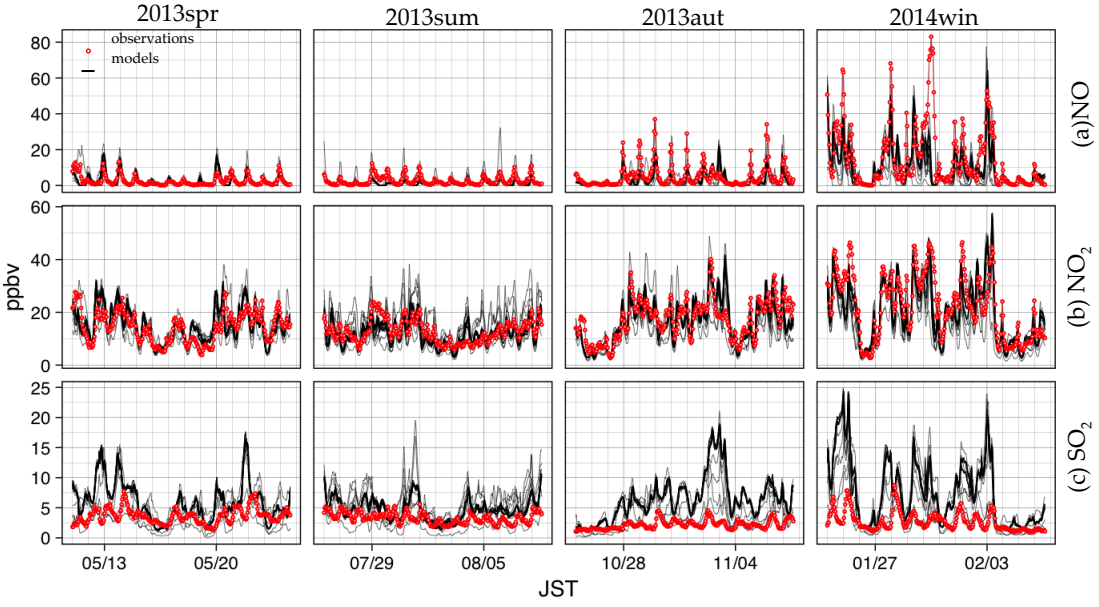

Figure 6. Spatial averages of observed and simulated hourly concentrations for (**a**) NO, (**b**) nitrogen dioxide (NO_2), and (**c**) sulfur oxide (SO_2) from different AAPMSs within d03 over the four seasons.

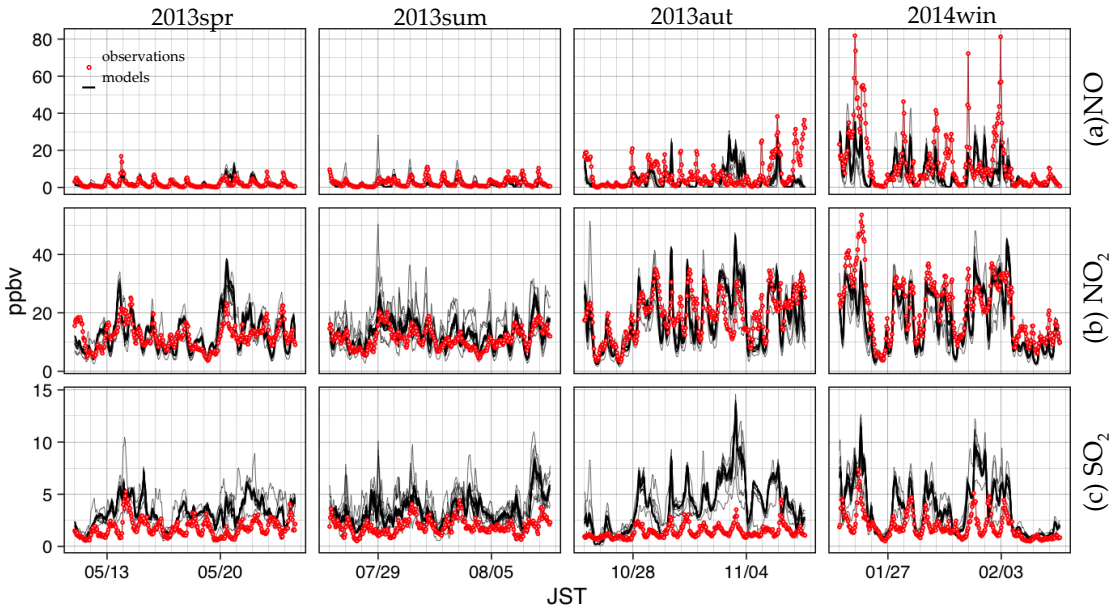

Figure 7. Spatial averages of observed and simulated hourly concentrations for (**a**) NO, (**b**) NO_2, and (**c**) SO_2 from different AAPMSs within d04 over the four seasons.

Table 3. Observed and simulated averaged concentrations [1] and ensemble performances [2] of the participant CTMs for hourly concentrations of NO, NO_2, and SO_2 at each AAPMS in each season.

	MEAN		NMB	Correl	IoA	N	MEAN		NMB	Correl	IoA	N
	[μg/m^3]		[%]				[μg/m^3]		[%]			
	Observation	Model					Observation	Model				
			d03						d04			
2013spr												
NO	2.53	2.53	8.3	0.38	0.48	24	2.53	2.53	58.26	0.37	0.50	22
NO_2	14.49	15.02	0.4	0.37	0.58	24	14.49	15.02	7.13	0.38	0.56	22
SO_2	3.61	5.70	120.0	0.33	0.42	17	3.61	5.70	128.23	0.33	0.46	20
2013sum												
NO	2.59	1.05	−53.0	0.43	0.50	24	5.10	3.00	−42.53	0.40	0.49	23
NO_2	12.75	12.31	−3.1	0.37	0.58	24	17.32	16.20	14.71	0.41	0.58	23
SO_2	3.28	4.78	189.0	0.19	0.35	16	2.18	5.98	119.09	0.28	0.40	20
2013aut												
NO	5.10	3.00	−36.2	0.34	0.47	24	2.59	1.05	−43.13	0.18	0.41	23
NO_2	17.32	16.20	−8.1	0.47	0.64	24	12.75	12.31	−4.94	0.45	0.64	23
SO_2	2.18	5.98	353.6	0.32	0.26	17	3.28	4.78	449.61	0.31	0.30	20
2014win												
NO	15.16	9.62	−41.5	0.31	0.51	24	15.16	9.62	−42.15	0.28	0.49	23
NO_2	22.55	19.50	−16.1	0.56	0.72	24	22.55	19.50	−19.40	0.54	0.71	23
SO_2	2.71	7.02	233.6	0.40	0.37	17	2.71	7.02	138.96	0.33	0.38	20

[1] Observation MEAN calculated from hourly value at each AAPMS in d03 and d04 for each season, respectively. Model MEAN calculated from seasonal averages from hourly value in each CTM corresponding to available observations at each AAPMS in d03 and d04. [2] Ensemble means of NMB (normalized mean bias), Correl (correlation coefficient), IoA (index of agreement), N (the number of available observation stations) calculated from all pairs of observations and simulations for each AAPMS and CTM in d03 and d04, respectively.

In general, most CTMs showed good agreement with the observed concentration levels of NO and NO_2 for each season, with regular diurnal patterns of NO in the warmer seasons. However, none of the models fully reproduced the elevated concentrations, e.g., for 19–20 May and 3 November (NO and NO_2) and 30 January (NO), with differences of 50%–200% between the observations and models, among others; the models tend to overestimate the observed daily maximums of NO: around 10–20 ppbv in spring and around 10–30 ppbv in summer, by a factor of 2.

For midnight on 30 January, all participant CTMs could not simulate the considerably increased level of NO before the rapid NO decrease associated with airmass changes, although all participants

reproduced the NO decrease well. This suggests that CTMs successfully simulated the concentration change owing to meteorological changes in the synoptic scale but failed to simulate an increase in the amounts owing to local scale meteorological changes such as the strong atmospheric stability, especially during colder seasons. All models tended to overevaluate the daytime NO reduction. In particular, two WRF-Chem types (M30 and M31) and M05 produced strikingly low constant values, 0.001 or 0.000 ppbv, during the daylight hours in summer and autumn. The normalized mean bias (NMB) for both domains produced a strong underestimation of NO (approximately −40% to −50%), except during the spring. Underestimates of NO at remote stations in Japan have been observed for regional CTMs, as reported by MICS–Asia III results [9], and the correlations and index of agreement (IoA) values ranged from 0.18 to 0.43 and 0.41 to 0.51, respectively. The performance levels of each model exhibited substantial differences between both domains and seasons. The differences between seasons are likely related to meteorology simulation abilities, but the reasons for the differences appearing between domains are unclear in this stage.

The differences for NO_2 in each model were large. Among these models, M31, M32, and M30 tended to overestimate elevated NO_2 levels. The lower levels of NO_2 obtained by M30 were often comparable to the NO_2 concentration obtained by M03, which provided considerably lower NO_2 concentrations compared to other models. These results suggest that the differences in meteorological conditions and NO_x chemistry in each model produced the NO_2 discrepancy between the models. Most of the models produced better results for NO_2 than for NO, with ensemble averages of seasonal statistics, e.g., correlation values, of 0.56 (d03) and 0.55 (d04), 0.72 (d03), and 0.71 (d04), particularly in the winter.

Over the year, most models obviously overestimated the observed SO_2, with an ensemble bias of 1.7–4.2 ppbv (NMB: 120%–350%) for d03 and 1.5–2.5 ppbv (NMB: 160%–470%) for d04. In addition, relatively high SO_2 levels were found for M30, M31, and M32. Meanwhile, M03 and M20 tended to produce lower concentrations compared to the other models, with a negative bias of −1.3 ppbv (M03) and −0.2 ppbv (M20) recorded especially in the spring; and exhibited better performances (IoA: 0.58–0.59) over the other models (IoA: 0.30–0.39), especially in the winter. The input SO_2 emissions into two CMAQ simulations (M03 and M20) differed from SO_2 emissions of J-STREAM. For example, SO_2 emissions in both total and bottom layers of J-STREAM were more than twice those of M03 for d03, respectively. Meanwhile, for d04, including active volcanos, although the total SO_2 emissions of J-STREAM were half those of M03, the bottom layer SO_2 emissions of J-STREAM were 1.3 times those of M03. The differences in divided SO_2 emission amounts in the lower layers possibly affected the simulated atmospheric SO_2 concentrations. The second-best model setting, M03, performed slightly better (IoA: 0.41) than other models, which suggests that atmospheric SO_2 concentrations were considerably affected by the input emission conditions, including the injection heights. Although modifications of emission conditions help to produce better SO_2 simulation, using modifications alone to resolve the overestimation of SO_2 (up to 470%) is not realistic.

The differences among models with respect to emissions, chemistries, and meteorological conditions led to major differences in simulated primary pollutant concentrations; moreover, the simulated differences between similar model settings increased in the winter.

4.2. Simulated Daily Concentrations of $PM_{2.5}$ Components and Total $PM_{2.5}$ Mass

Figures 8 and 9 present spatially averages obtained from observed and simulated daily concentrations for $PM_{2.5}$ components (SO_4^{2-}, NO_3^-, NH_4^+, EC, and OC) and total $PM_{2.5}$ mass for different AAPMSs in d03 and d04, respectively. The seasonal ensemble performances of the participant CTMs at each AAPMS are also summarized as statistics in Tables 4 and 5 for each domain. The goal and criteria levels for CTM performance statistics, NMB, normalized mean error (NME), and correlation were recommended by Emery et al. [52], and the fractional bias (FB) and fractional error (FE) were recommended by Boylan and Russell [53], which is listed in Table A1. Individual model performance reports of each CTM are shown in Tables A2 and A3.

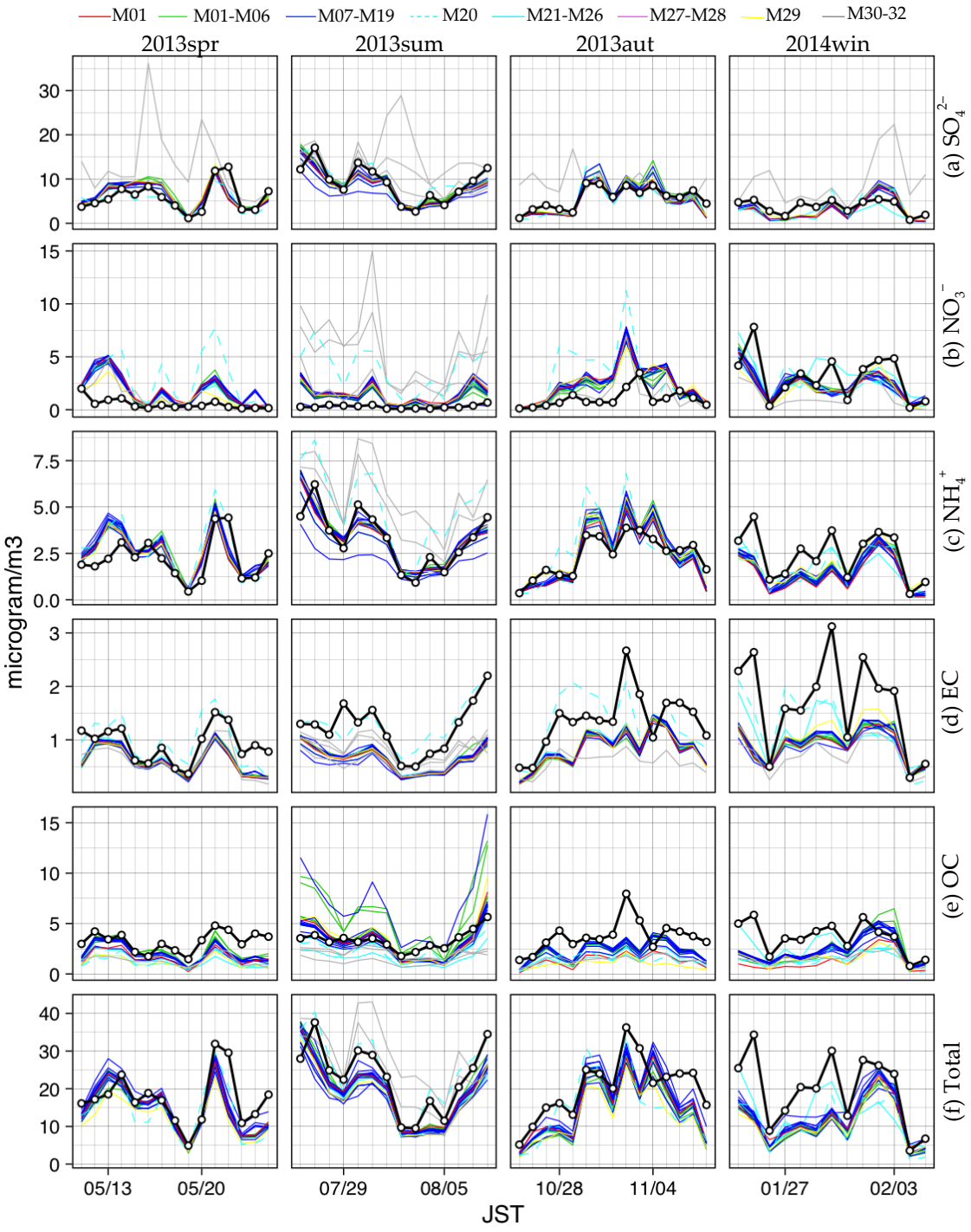

Figure 8. Spatially averaged concentrations of $PM_{2.5}$: (**a**) SO_4^{2-}, (**b**) NO_3^-, (**c**) NH_4^+, (**d**) EC, (**e**) OC, and (**f**) total $PM_{2.5}$ mass over the four seasons. These results are based on daily concentrations observed and simulated for AAPMSs in d03. The thick solid lines with open circles present observations, and the colored lines present model results.

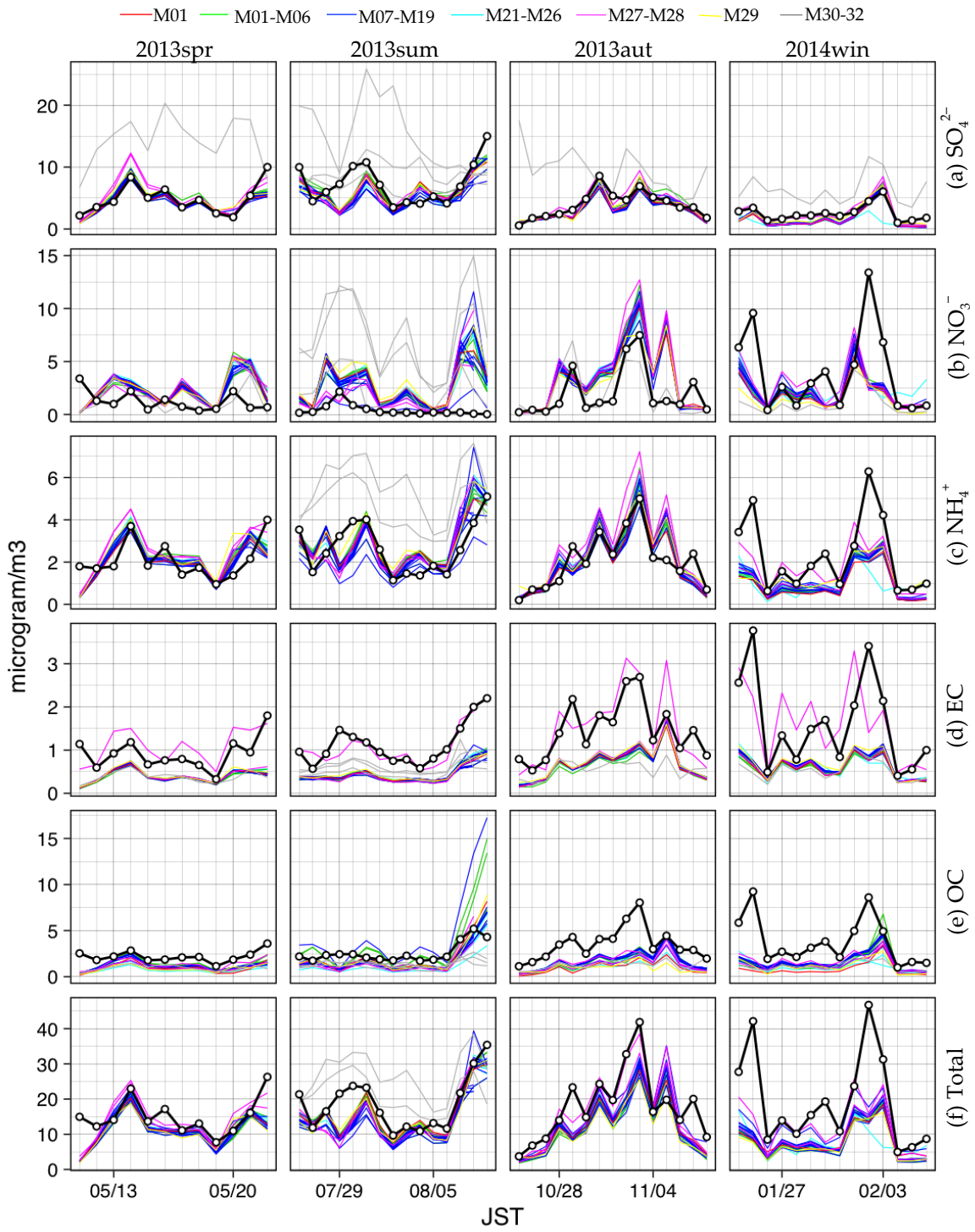

Figure 9. Spatially averaged concentrations of $PM_{2.5}$: (**a**) SO_4^{2-}, (**b**) NO_3^-, (**c**) NH_4^+, (**d**) EC, (**e**) OC, and (**f**) total $PM_{2.5}$ over the four seasons. These results are based on daily concentrations observed and simulated for AAPMSs in d04. The thick solid lines with open circles present observations, and the colored lines present model results.

Table 4. Observed and simulated averaged concentrations [1] and ensemble performances [2] of the participant CTMs for daily concentrations of total $PM_{2.5}$ and $PM_{2.5}$ components at each AAPMS within d03.

	MEAN		MB	ERROR	RMSE	NMB	NME	FB	FE	Correl	IoA	N
	[μg/m^3]		[μg/m^3]	[μg/m^3]	[μg/m^3]	[%]	[%]	[%]	[%]			
	Observation	Model										
2013spr												
SO_4^{2-}	5.87	6.59	1.68	2.23	2.95	32.44	41.39	25.75	34.46	0.77	0.79	19
NO_3^-	0.52	1.72	1.44	1.61	2.22	310.08	333.28	72.92	109.94	0.44	0.34	18
NH_4^+	2.21	2.54	0.65	0.96	1.21	32.01	45.82	26.86	39.52	0.70	0.74	19
EC	0.92	0.63	−0.20	0.31	0.39	−22.33	33.40	−27.91	38.94	0.73	0.71	18
OC	3.23	1.85	−1.06	1.21	1.42	−32.46	39.30	−45.81	52.95	0.70	0.67	18
TOTAL	17.33	14.58	−0.99	3.95	4.90	−5.30	22.60	−9.00	25.53	0.81	0.86	19
2013sum												
SO_4^{2-}	9.11	8.84	0.04	2.68	3.50	1.65	30.34	3.66	30.41	0.74	0.82	20
NO_3^-	0.28	1.73	1.22	1.30	1.73	650.97	672.36	98.26	122.69	0.32	0.21	19
NH_4^+	3.32	3.49	0.23	1.16	1.46	8.47	35.92	8.92	34.28	0.73	0.79	20
EC	1.23	0.69	−0.45	0.49	0.56	−38.53	42.31	−50.07	54.86	0.67	0.62	20
OC	3.35	3.28	−0.01	1.34	1.60	6.75	47.22	−11.01	45.68	0.65	0.58	20
TOTAL	23.07	19.71	−2.93	5.96	7.33	−12.77	26.30	−16.97	29.10	0.78	0.82	20
2013aut												
SO_4^{2-}	5.73	5.46	−0.21	1.73	2.12	0.50	29.11	−13.77	34.68	0.86	0.87	18
NO_3^-	1.05	2.33	1.55	1.96	2.70	193.57	233.81	54.87	103.17	0.28	0.31	16
NH_4^+	2.38	2.49	0.30	0.87	1.16	13.45	35.42	−2.69	34.45	0.86	0.83	18
EC	1.36	0.85	−0.50	0.65	0.78	−33.56	43.92	−44.22	55.76	0.43	0.56	18
OC	3.73	2.02	−1.78	2.03	2.43	−42.93	49.71	−57.62	67.42	0.44	0.51	18
TOTAL	20.27	15.36	−4.26	6.61	7.98	−19.16	30.78	−32.14	40.63	0.76	0.79	18
2014win												
SO_4^{2-}	3.75	3.31	−0.39	2.00	2.41	−8.85	52.14	−35.89	61.17	0.66	0.68	21
NO_3^-	3.08	2.31	−0.89	1.86	2.55	−18.85	57.79	−18.48	68.65	0.37	0.60	21
NH_4^+	2.40	1.51	−0.94	1.05	1.30	−34.93	39.89	−48.01	53.60	0.75	0.74	21
EC	1.69	0.94	−0.90	0.96	1.19	−45.98	50.26	−52.36	62.90	0.55	0.58	19
OC	3.62	2.07	−1.72	2.13	2.53	−35.59	57.36	−52.86	73.17	0.43	0.53	21
TOTAL	19.57	11.69	−8.66	9.12	11.21	−40.43	43.05	−52.25	55.77	0.67	0.65	21

[1] Observation MEAN calculated from daily value at each AAPMS in d03 for each season. Model MEAN calculated from seasonal averages from daily value in each CTM corresponding to available observations at each AAPMS in d03. [2] Ensemble mean of MB (mean bias), ERROR (mean error), RMSE (root mean square error), NMB (normalized mean bias), NME (normalized mean error), FB (fractional bias), FE (fractional error), Correl (correlation coefficient), IoA (index of agreement), N (the number of available observation stations) calculated from all pairs of observation and simulation for each AAPMS and CTM in d03. Observation data from valid AAPMSs that obtained data for each $PM_{2.5}$ component over a period of at least eight days (53%) from each target period (up to 15 days) per each station were used to evaluate the performances (MB, ERROR, RMSE, NMB, NME, FB, FE, Correl, and IoA) of the participant CTMs.

Table 5. Observed and simulated averaged concentrations [1] and ensemble performances [2] of the participant CTMs for daily concentrations of total $PM_{2.5}$ and $PM_{2.5}$ components at each AAPMS within d04.

	MEAN		MB	ERROR	RMSE	NMB	NME	FB	FE	Correl	IoA	N
	[μg/m^3]		[μg/m^3]	[μg/m^3]	[μg/m^3]	[%]	[%]	[%]	[%]			
	Observation	Model										
2013spr												
SO_4^{2-}	4.82	4.91	0.39	1.57	1.93	10.98	35.85	0.35	33.74	0.80	0.84	20
NO_3^-	1.24	2.20	0.95	1.82	2.46	145.14	206.47	35.06	107.72	0.17	0.35	20
NH_4^+	2.10	2.14	0.15	0.78	1.01	9.44	39.89	2.42	41.05	0.57	0.72	20
EC	0.91	0.43	−0.39	0.46	0.54	−40.16	57.18	−59.42	73.42	0.44	0.51	19
OC	2.19	1.12	−0.94	1.07	1.22	−39.05	50.83	−59.38	70.61	0.45	0.49	19
TOTAL	15.02	11.47	−2.91	4.59	6.11	−19.01	32.18	−27.57	39.98	0.53	0.68	20
2013sum												
SO_4^{2-}	6.49	6.25	−0.68	2.82	3.54	−9.21	44.02	−13.08	44.10	0.36	0.57	22
NO_3^-	0.40	2.85	1.85	1.92	2.68	587.86	600.84	117.21	129.97	0.44	0.34	22
NH_4^+	2.66	2.88	0.13	0.99	1.26	6.98	42.50	5.58	38.98	0.56	0.67	22
EC	1.13	0.47	−0.57	0.60	0.67	−55.79	59.89	−79.59	84.08	0.44	0.45	22
OC	2.56	1.93	−0.81	1.08	1.23	−32.37	49.92	−49.81	63.83	0.10	0.39	22
TOTAL	18.61	15.18	−3.35	5.97	7.36	−19.73	36.69	−25.14	41.25	0.52	0.61	22

Table 5. *Cont.*

	MEAN		MB	ERROR	RMSE	NMB	NME	FB	FE	Correl	IoA	N
	[μg/m^3]		[μg/m^3]	[μg/m^3]	[μg/m^3]	[%]	[%]	[%]	[%]			
	Observation	Model										
2013aut												
SO_4^{2-}	3.91	3.66	−0.38	1.30	1.63	−7.51	30.43	−14.04	32.83	0.84	0.86	20
NO_3^-	2.00	3.36	1.99	2.82	3.90	171.39	206.12	55.45	95.32	0.54	0.56	20
NH_4^+	2.07	2.15	0.24	0.91	1.24	14.50	42.85	5.85	39.32	0.73	0.78	20
EC	1.46	0.72	−0.79	0.84	1.01	−49.30	53.29	−67.93	71.71	0.51	0.57	20
OC	3.53	1.53	−2.19	2.27	2.70	−56.03	58.42	−79.11	84.80	0.55	0.53	20
TOTAL	17.97	13.07	−4.49	6.97	8.99	−22.54	35.93	−32.02	43.51	0.71	0.76	20
2014win												
SO_4^{2-}	2.55	1.92	−0.60	1.19	1.34	−20.85	42.55	−48.72	60.94	0.88	0.84	19
NO_3^-	3.91	2.06	−2.36	3.04	4.54	−42.80	65.21	−38.83	78.53	0.37	0.55	19
NH_4^+	2.31	1.10	−1.40	1.46	1.99	−49.28	51.85	−64.33	67.79	0.70	0.65	19
EC	1.61	0.67	−1.05	1.11	1.46	−57.57	61.09	−70.06	76.46	0.48	0.52	19
OC	3.82	1.41	−2.77	3.03	3.90	−58.50	68.46	−74.99	96.14	0.36	0.48	19
TOTAL	19.26	8.45	−12.53	12.76	16.88	−55.14	56.41	−71.88	73.82	0.62	0.58	19

[1] Observation MEAN calculated from daily value at each AAPMS in d04 for each season. Model MEAN calculated from seasonal averages from daily value in each CTM corresponding to available observations at each AAPMS in d04. [2] E Ensemble means of MB (mean bias), ERROR (mean error), RMSE (root mean square error), NMB (normalized mean bias), NME (normalized mean error), FB (fractional bias), FE (fractional error), Correl (correlation coefficient), IoA (index of agreement), N (the number of available observation stations) calculated from all pair of observation and simulation for each AAPMS and CTM in d04. Observation data from valid AAPMSs that obtained data for each $PM_{2.5}$ component over a period of at least eight days (53%) from each target period (up to 15 days) per each station were used to evaluate the performances (MB, ERROR, RMSE, NMB, NME, FB, FE, Correl, and IoA) of the participant CTMs.

With SO_4^{2-} as a dominant $PM_{2.5}$ component, most CTMs showed good agreement with daily concentration levels and day-to-day changes in both domains for each season, with the exception of a few model settings. Overall, the ensemble statistics, including the NMB (−0.85, 1.65%), NME (30.34, 29.11), FB (3.66, −13.77%), FE (30.41, 34.28), and correlation (0.74, 0.86), passed the goal level in d03 for summer and autumn. For d04, the NMB (−7.5%), NME (30.34), FB (−13.04%), FE (32.83%), and correlation (0.84) passed the goal level for summer. With the exception of d03 in winter and d04 in summer, the correlation and IoA indicated excellent performance, with maximum values of 0.74–0.88 and 0.79–0.87 for d04 in winter. Most CTMs underestimated the observed SO_4^{2-} in d04 on 29–30 July, with relatively low values for the correlation (0.36) and IoA (0.52). This result may lead to underestimations of the total $PM_{2.5}$ mass in connection with the NH_4^+ concentrations. WRF-Chem (M30, 31) clearly overestimated SO_4^{2-} concentrations in $PM_{2.5}$ due to the SO_4^{2-} mass build-up problem associated with the nucleation calculation in MADE/SORGAM [54]. In addition, the WRF-Chem group employed their own physical parameterizations such as cumulus convection and microphysics for their meteorological simulations. Additional sensitivity simulations for meteorological fields are required to quantitatively evaluate the model inter-differences of SO_4^{2-} and total $PM_{2.5}$ mass concentrations owing to the differences in meteorological simulations. We will perform this in the next phase. The largest positive biases were found in M31, with 3.0–9.7 μg/m^3 (NMB: 52%–177%) for d03 and 3.8–10.2 μg/m^3 (NMB: 131%–240%) for d04. These simulated overestimations were slightly higher for CMAQ Version 4.7.1 (M27 and M28), particularly for d04 in spring. This trend indicates that the updated sulfur chemistries in CMAQ Version 5.0 [35,55–58] enhanced the performance of this model compared to the previous versions. In winter, CAMx (M29) performed better, with biases of −0.32 μg/m^3 (NMB: −7.3%) for d04 and 0.39 μg/m^3 (NMB: 3.4%) for d04 under the same emission condition. This result is attributed to an underestimation of SO_4^{2-} by the dominant participant model, CMAQ, which may be caused by an inadequate aqueous-phase SO_4^{2-} production by Fe- and Mn-catalyzed O_2 oxidation [14].

All participant CTMs overestimated NO_3^- levels in warmer seasons, with ensemble biases of 1.22–1.55 μg/m^3 (NMB: 194%–651%) for d03 and 0.85–1.99 μg/m^3 (NMB: 145%–588%) for d04. The largest positive biases were found in summer. Above all, M20, M30, and M31 strongly overestimated elevated NO_3^-levels. Only M11 showed relatively good agreement with observations for d03 in

summer, with a minimum bias of 0.12 μg/m^3 (NMB: 91%) and improved values for the correlation (0.46) and IoA (0.54). However, M11 also produced low concentrations for SO_4^{2-} and NH_4^+. As observed for d04 in autumn, all models exhibited better performance for the daily concentration levels and day-to-day changes in NO_3^-. For example, M30 has a minimum bias of 0.14 μg/m^3 (NMB: 11%), which passed the goal NMB level for 24-h NO_3^-. Some deviations in NO_3^- between observations and the models were attributed to NH_4^+ and potentially NH_4NO_3. In winter, most models reproduced day-to-day changes in both domains but tended to underestimate elevated NO_3^- levels, with ensemble mean biases of −0.89 μg/m^3 (NMB: −18.9%) and −2.36 μg/m^3 (NMB: −42.8%). A previous model inter-comparison study for the Tokyo metropolitan area, UMICS, concluded that the participant models overestimated NO_3^- levels in both summer and winter [11,12], although available observations included only one winter and three summer stations. In our validations, most models produced higher NO_3^- levels in spring and summer, lower NO_3^- levels in winter, and moderate NO_3^- levels in autumn, compared with accumulated observation data for d03 and d04. This result is expected to be more accurate than previous reports because a greater number of observations (for 18–22 stations) were included.

As mentioned above, the day-to-day variations in NH_4^+ were consistent with those of SO_4^{2-} and NO_3^-. Therefore, most CTMs showed good agreement with daily concentration levels and day-to-day changes in both domains for each season, with the exception of some elevated peaks. Above all, the ensemble performances indicators, FE and FB, were −27.9%–8.9% and 34.3%–41.1%, thus passing the goal level in both domains for all seasons except winter. Notably, the differences among models increased in summer. Two WRF-Chem models (M32, M31) predicted higher NH_4^+ levels, with biases of 1.96–3.03 μg/m^3 (NMB: 84%–130%) and 1.72–2.71 μg/m^3 (NMB: 85%–61%) for d03 and d04, respectively. The M20 model, which employed EAGrid for emissions and an original configuration for meteorology, also produced relatively high NH_4^+ levels in d03, with a bias of 1.68 μg/m^3 (NMB: 51%). These overpredictions were likely associated with those of SO_4^{2-} and NO_3^- in summer. Meanwhile, relatively larger negative biases were found for M11, at −1.18 μg/m^3 (NMB: 35%) for d03 and −0.81 μg/m^3 (NMB: 33%) for d04.

The EC levels simulated by most CTMs were considerably lower than the observations in both domains for all season. The model ensemble biases were −0.90 to −0.20 μg/m^3 (NMB: −46% to −22%) and −2.77 to −0.39 μg/m^3 (NMB: −58% to −40%) for d03 and d04, respectively, with larger values for Tokyo. Both models employing EAGrid2000-JAPAN (M20 (d03) and M27 (d04)) produced higher EC values than other CTMs with different emission settings, and relatively better NMB values were obtained, at −20% to −3% and −35% to 42%, respectively. This trend suggests that the EC emissions of J-STREAM might be underestimated.

The CTMs reproduced some of elevated OC levels in the warmer seasons, but clearly underestimated the observed OC levels for autumn and winter, with model ensemble biases of −1.78 to −0.01 μg/m^3 (NMB: −42% to 7%) and −2.77 to −0.81 μg/m^3 (NMB: −59% to −39%) for d03 and d04, respectively, which are similar to the EC values. Additionally, as observed for the EC, the negative biases of OC for the Tokyo area were larger than those for western Japan. However, the negative biases of all participant CTMs have been clearly moderated compared with the UMICS cases [11,12]. Among the models, M02, M03, and M11 predicted relatively higher OC levels and overestimated the summer OC concentrations. Full-domain nesting simulations were performed via M02 and M03 using a relatively recent CMAQ model (Version 5.1), which includes updates for some chemical and aerosol mechanisms, such as POA aging, SOA mass yields with new pathways from isoprene, alkanes, and PAHs, and SOA formation reactions in the aqueous-phase chemistry. Continual nesting simulations for the Asian scale (d01) performed by CMAQ Version 5.1 exhibited higher regional-scale OC levels, leading to higher OC levels in urban areas in Japan compared with previous versions. Thus, an empirical SOA yield model can predict the same OC concentration level as the VBS model M11. It should be noted that effect of the updated SOA yield mechanisms was not clear at the urban scale

when using CMAQ Version 5.1 or higher (e.g., M01, M04–05). Additionally, to evaluate simulated OC concentrations, more observational data are needed.

Overall, most CTMs showed good agreement with observed concentration levels of total $PM_{2.5}$ mass in both domains for each season. These results are likely associated with the reproducibility of some dominant components, e.g., SO_4^{2-} and NH_4^+. Moreover, CTMs tended to fail at reproducing some heavily polluted situations and underestimated the considerably high $PM_{2.5}$ concentrations (approximately 40–50 μg/m^3). A considerable underestimation (≈30 μg/m^3) of total $PM_{2.5}$ associated with $PM_{2.5}$ components, except for SO_4^{2-}, was observed for d04 in the winter season, 25 January and 2 February; during that time, the nighttime simulated surface temperature was clearly lower than that in the observations (Figure 3). This implies that the simulated higher surface temperature compared with that in the observations formed weaker atmospheric stability, which produced weaker accumulations of particulate pollutants at nighttime, especially during colder seasons. The model ensemble biases were −8.66 to −0.99 μg/m^3 (NMB: −43% to −5%) for d03 and −2.91 to −11.98 μg/m^3 (NMB: −55% to −19%) for d04. The largest negative biases are found in winter due to underestimations of NH_4NO_3, particularly for d04. M31 and M32 tended to overpredict the total $PM_{2.5}$ due to overestimates of inorganic compounds. Of the model ensemble statistics for d03, the NMB (−5%, 13%) NME (22%, 26%), FB (−9%, −17%), FE (26%, 29%), and correlation (0.81, 0.78) passed the goal level for 24-h total $PM_{2.5}$ mass in spring and summer, respectively. In addition, the majority of the other statistical indicators passed the criteria levels as well.

5. Summery

A model inter-comparison of secondary pollutant simulations over urban areas in Japan, J-STREAM Phase I, was performed, in which a total of 32 simulations were conducted by combining CMAQ, CAMx, and WRF-Chem.

Simulated hourly concentrations of the primary pollutants NO and NO_2, which are precursors of $PM_{2.5}$, generally showed good agreement with the observed concentrations, at the same level as the MICS case. However, some differences between observations and simulations and CTMs may be considered to be caused by the differences in meteorological conditions and NOx chemistries of each CTM. Furthermore, most of the CTMs using the same input emissions tended to overestimate SO_2 concentrations, although the models showed good performance for $PM_{2.5}$ SO_4^{2-}. The different emission inventory, EAGrid produced better results for SO_2; therefore, it appears that the emission input can be improved. However, it was likely to be unrealistic that just the modifications of the emissions could fully resolve the overestimation of SO_2.

Simulated concentrations of $PM_{2.5}$ and its components were evaluated via a comparison with daily observed concentrations by using the filter pack method at selected AAPMSs for a period of at least two weeks for each season in this project. In general, most of the models showed good agreement with the observed concentration of total $PM_{2.5}$ mass for each season, within goal or criteria levels of model ensemble statistics especially in warmer seasons. This agreement was associated with the reproducibility of some of dominant particulates.

Among individual $PM_{2.5}$ components, most model results for SO_4^{2-} and NH_4^+ showed good agreement with daily concentration levels and day-to-day variations, with good model ensemble statistics, particularly for the warmer seasons. However, for SO_4^{2-}, a problem in the WRF-Chem model and novel, improved mechanisms for SO_4^{2-} formation in most CTMs were found through this model inter-comparison. Additionally, we found that the differences in the Asian scale precipitation patterns between precipitation parametrizations affected the simulated water-soluble $PM_{2.5}$ concentrations. Additional improvements for SO_4^{2-} were expected, particularly for the winter [11]. All participant models showed a strong tendency to overestimate NO_3^- in warmer seasons, with the model ensemble NMB reaching 651%. However, in winter, most of the models reproduced the day-to-day variations, with underestimations for elevated NO_3^- levels. These tendencies differed from a previous model inter-comparison, UMICS, which concluded that the participant models overestimated NO_3^- levels

in both summer and winter [11,12]. This difference between two model inter-comparison studies is attributed to variations in the number of observations applied for verification. Thus, a sufficient amount of observation data on $PM_{2.5}$ components is needed to evaluate and improve CTMs. The EC levels simulated by most models were considerably lower than the observed levels for all seasons; however, some models employing EAGrid emissions produced higher EC levels than the other models. The models reproduced concentrations for some elevated OC values in the warmer seasons, but clearly underestimated the OC levels in autumn and winter. In addition, some models employing the VBS model and the newly updated SOA yield mechanisms produced higher OC levels and even overestimated the observed OC concentration in some cases.

This study has identified some effective approaches for improving $PM_{2.5}$ simulations for urban areas in Japan based on a model inter-comparison. First, improvements in emissions are expected to increase the reproducibility of primary pollutants that are precursors of $PM_{2.5}$ and EC concentrations. For SO_4^{2-}, NO_3^-, and OC, additional formation pathways can help to reduce underestimations. The recent model updates (e.g., CMAQ Version 5.3) improved the chemical pathways and are expected to simulate the secondary $PM_{2.5}$ components well. Simulated meteorological fields will be important for the Asian scale $PM_{2.5}$ concentration levels and the elevated $PM_{2.5}$ concentrations during the days with high amounts of pollution. In addition, special attention is needed for misjudgments in these models. Finally, additional accumulated observations are needed to evaluate the simulated concentrations. Future studies will include these modifications to realize reference air quality modeling in the next stages of J-STREAM.

Author Contributions: K.Y. managed the model inter-comparison (J-STREAM), prepared the initial, boundary, and meteorological inputs, and wrote this article. S.C. is the leader of J-STREAM project and prepared emission inputs. S.I. and H.H. are core members of J-STREAM in charge of inorganic aerosols. T.S. is a core member of J-STREAM in charge of photochemical gases. M.S., M.T., T.M. (Tazuko Morikawa), I.K., Y.M. (Yukako Miya), H.K., Y.M. (Yu Morino), K.K., T.N., H.S., K.U., and Y.F. are participants who conducted the model simulations. T.H. and T.M. (Takeshi Misaki) analyzed the submitted data. K.S. is in charge of global simulations. All authors have read and agreed to the published version of the manuscript.

Funding: This research was funded by the Environment Research and Technology Development Fund (5-1601) of the Environmental Restoration and Conservation Agency, JSPS KAKENHI Grant Number 18H03369, and the Collaborative Research Program of Research Institute for Applied Mechanics, Kyushu University.

Acknowledgments: This project was supported by the Environment Research and Technology Development Fund (5-1601) of the Environmental Restoration and Conservation Agency. This work was also partially supported by JSPS KAKENHI Grant Number 18H03369. Monitoring data of APMSs were obtained from National Institute for Environmental Studies. This work was supported in part by the Collaborative Research Program of Research Institute for Applied Mechanics, Kyushu University.

Conflicts of Interest: The authors declare no conflict of interest.

Appendix A

Table A1. Recommended benchmarks for photochemical model performance statistics [52,53].

	NMB		NME		r		FB		FE	
Species	**Goal**	**Criteria**	**Goal**	**Criteria**	**Goal**	**Criteria**	**Goal**	**Criteria**	**Goal**	**Criteria**
24-h $PM_{2.5}$, SO_4^{2-}, NH_4^+	<±10%	<±30%	<35%	<50%	>0.70	>0.40				
24-h NO_3^-	<±15%	<±65%	<65%	<115%	None	None	<±30%	<±60%	<±60%	<±75%
24-h OC	<±15%	<±50%	<45%	<65%	None	None				
24-h EC	<±20%	<±40%	<50%	<75%	None	None				

Table A2. Individual model performance (IoA) for d03.

ID	2013Spr						2013Sum					
	SO_4^{2-}	NO_3^-	NH_4^+	EC	OC	TOTAL	SO_4^{2-}	NO_3^-	NH_4^+	EC	OC	TOTAL
M01	0.82	0.32	0.74	0.71	0.62	0.86	0.84	0.19	0.80	0.60	0.62	0.83
M02	0.80	0.35	0.74	0.73	0.76	0.87	0.84	0.24	0.81	0.62	0.39	0.84
M03	0.81	0.34	0.75	0.74	0.70	0.88	0.85	0.23	0.82	0.59	0.34	0.83
M04	0.81	0.36	0.74	0.71	0.73	0.86	0.83	0.23	0.80	0.61	0.64	0.83
M05	0.80	0.33	0.72	0.72	0.74	0.86	0.84	0.22	0.80	0.62	0.63	0.83
M06	0.85	0.35	0.76	0.69	0.71	0.85	0.82	0.25	0.80	0.57	0.65	0.78
M07	0.82	0.35	0.75	0.71	0.70	0.85	0.87	0.23	0.83	0.65	0.61	0.86
M08	0.82	0.33	0.74	0.73	0.72	0.86	0.86	0.20	0.81	0.63	0.64	0.83
M09	0.83	0.33	0.75	0.73	0.72	0.86	0.84	0.20	0.81	0.63	0.64	0.82
M10							0.84	0.20	0.81	0.62	0.64	0.82
M11							0.69	0.43	0.66	0.54	0.30	0.76
M12	0.80	0.32	0.72	0.73	0.73	0.86	0.86	0.19	0.81	0.62	0.63	0.84
M13	0.81	0.34	0.70	0.73	0.62	0.86	0.85	0.19	0.80	0.63	0.64	0.83
M14	0.83	0.33	0.74	0.72	0.72	0.85	0.86	0.21	0.82	0.63	0.64	0.79
M15	0.83	0.33	0.74	0.72	0.71	0.87	0.86	0.21	0.82	0.62	0.64	0.84
M16							0.85	0.21	0.81	0.62	0.64	0.82
M17							0.85	0.20	0.81	0.62	0.64	0.83
M18							0.85	0.20	0.81	0.62	0.64	0.83
M19							0.85	0.20	0.80	0.62	0.63	0.83
M20	0.84	0.20	0.69	0.70	0.55	0.81	0.85	0.07	0.71	0.63	0.59	0.84
M21	0.82	0.32	0.73	0.72	0.72	0.85	0.85	0.19	0.81	0.63	0.64	0.83
M22	0.82	0.32	0.74	0.73	0.59	0.86	0.85	0.21	0.81	0.62	0.62	0.82
M23	0.84	0.36	0.76	0.71	0.70	0.87	0.86	0.22	0.82	0.62	0.64	0.83
M24	0.84	0.36	0.76	0.71	0.70	0.87	0.86	0.22	0.82	0.62	0.64	0.83
M26	0.83	0.37	0.73	0.71	0.50	0.87	0.86	0.21	0.81	0.62	0.50	0.81
M29	0.81	0.42	0.75	0.71	0.54	0.80	0.86	0.22	0.81	0.62	0.59	0.81
M30	0.27	0.32		0.66	0.50		0.36	0.22	0.57	0.54	0.42	0.69
M31							0.68	0.06	0.70	0.69	0.54	0.83
M32							0.84	0.07		0.68	0.52	
ID	**2013Aut**						**2013Win**					
	SO_4^{2-}	NO_3^-	NH_4^+	EC	OC	TOTAL	SO_4^{2-}	NO_3^-	NH_4^+	EC	OC	TOTAL
M01	0.91	0.30	0.85	0.85	0.46	0.79	0.69	0.60	0.69	0.55	0.45	0.61
M02	0.89	0.35	0.83	0.83	0.56	0.77	0.70	0.57	0.74	0.57	0.53	0.63
M03	0.84	0.38	0.80	0.80	0.50	0.77	0.70	0.57	0.76	0.57	0.47	0.63
M04	0.90	0.34	0.85	0.85	0.53	0.79	0.69	0.57	0.71	0.55	0.53	0.64
M05	0.90	0.32	0.84	0.84	0.54	0.80	0.69	0.58	0.72	0.56	0.53	0.65
M06	0.90	0.32	0.85	0.85	0.51	0.77	0.70	0.58	0.68	0.55	0.53	0.62
M07	0.91	0.29	0.84	0.84	0.52	0.80	0.69	0.51	0.69	0.52	0.51	0.64
M08	0.90	0.30	0.83	0.83	0.54	0.80	0.71	0.63	0.75	0.58	0.55	0.67
M09	0.90	0.30	0.83	0.83	0.54	0.80	0.69	0.61	0.74	0.58	0.55	0.67
M10												
M11							0.42	0.26	0.39	0.44	0.31	0.40
M12	0.89	0.29	0.80	0.80	0.55	0.81	0.71	0.60	0.76	0.58	0.56	0.69
M13	0.86	0.33	0.79	0.79	0.49	0.81	0.71	0.58	0.77	0.58	0.53	0.67
M14	0.91	0.31	0.83	0.83	0.55	0.76	0.70	0.61	0.74	0.58	0.54	0.62
M15	0.91	0.30	0.84	0.84	0.54	0.80	0.70	0.61	0.74	0.57	0.54	0.66
M16												
M17												
M18												
M19												
M20	0.88	0.19	0.70	0.70	0.49	0.74	0.71	0.56	0.78	0.65	0.50	0.67
M21	0.91	0.29	0.83	0.83	0.56	0.80	0.68	0.57	0.69	0.63	0.60	0.65
M22	0.90	0.30	0.83	0.83	0.48	0.80	0.46	0.03	0.34	0.44	0.35	0.35

Table A2. *Cont.*

ID	2013Aut						2013Win					
	SO_4^{2-}	NO_3^-	NH_4^+	EC	OC	TOTAL	SO_4^{2-}	NO_3^-	NH_4^+	EC	OC	TOTAL
M23	0.90	0.33	0.85	0.85	0.53	0.79	0.69	0.60	0.71	0.57	0.54	0.64
M24	0.90	0.34	0.85	0.85	0.53	0.79	0.69	0.60	0.71	0.57	0.54	0.64
M26	0.90	0.33	0.84	0.84	0.44	0.79	0.70	0.58	0.73	0.57	0.49	0.64
M29	0.91	0.32	0.83	0.83	0.44	0.74	0.70	0.62	0.72	0.60	0.50	0.61
M30	0.30	0.36			0.44		0.27	0.52		0.53	0.48	
M31							0.72	0.19	0.31	0.41	0.33	0.46
M32							0.42	0.11	0.31	0.40	0.32	0.36
M31												
M32												

Table A3. Individual model performance (IoA) for d04.

ID	2013Spr						2013Sum					
	SO_4^{2-}	NO_3^-	NH_4^+	EC	OC	TOTAL	SO_4^{2-}	NO_3^-	NH_4^+	EC	OC	TOTAL
M01	0.86	0.34	0.71	0.50	0.48	0.67	0.59	0.33	0.71	0.44	0.38	0.64
M02	0.88	0.38	0.76	0.52	0.53	0.69	0.59	0.34	0.71	0.44	0.29	0.63
M03	0.86	0.39	0.74	0.51	0.53	0.70	0.61	0.38	0.70	0.43	0.27	0.62
M04	0.87	0.35	0.72	0.51	0.51	0.69	0.63	0.32	0.73	0.44	0.41	0.67
M05	0.87	0.35	0.72	0.51	0.50	0.68	0.62	0.33	0.72	0.44	0.41	0.66
M06	0.86	0.36	0.71	0.50	0.48	0.64	0.56	0.40	0.68	0.43	0.41	0.59
M07	0.86	0.38	0.72	0.51	0.50	0.70	0.62	0.37	0.71	0.43	0.38	0.61
M08	0.87	0.35	0.71	0.51	0.51	0.67	0.56	0.36	0.66	0.44	0.39	0.60
M09	0.87	0.37	0.73	0.51	0.51	0.67	0.56	0.37	0.66	0.44	0.39	0.60
M10							0.57	0.35	0.67	0.44	0.41	0.61
M11							0.52	0.54	0.56	0.44	0.28	0.52
M12	0.88	0.35	0.71	0.51	0.52	0.68	0.56	0.34	0.66	0.44	0.39	0.60
M13	0.88	0.36	0.70	0.51	0.47	0.67	0.55	0.34	0.68	0.44	0.39	0.62
M14	0.88	0.34	0.73	0.51	0.51	0.67	0.56	0.34	0.66	0.44	0.40	0.58
M15	0.88	0.34	0.73	0.51	0.51	0.70	0.55	0.34	0.66	0.44	0.39	0.59
M16							0.57	0.34	0.67	0.44	0.41	0.61
M17							0.57	0.35	0.67	0.44	0.41	0.61
M18							0.58	0.33	0.68	0.44	0.41	0.62
M19							0.57	0.33	0.69	0.44	0.40	0.63
M21	0.88	0.34	0.72	0.51	0.50	0.68	0.57	0.35	0.67	0.44	0.41	0.61
M22	0.88	0.34	0.72	0.51	0.45	0.68	0.57	0.35	0.67	0.44	0.40	0.62
M23	0.88	0.36	0.74	0.51	0.51	0.70	0.58	0.33	0.69	0.43	0.40	0.62
M24	0.88	0.36	0.75	0.51	0.51	0.70	0.58	0.34	0.69	0.43	0.40	0.62
M25	0.89	0.36	0.73	0.51	0.46	0.71	0.55	0.37	0.69	0.42	0.38	0.61
M26	0.88	0.35	0.72	0.51	0.42	0.69	0.57	0.32	0.70	0.43	0.36	0.63
M27	0.79	0.38	0.67	0.54	0.53	0.68	0.60	0.41	0.71	0.56	0.44	0.63
M28	0.82	0.34	0.66	0.52	0.47	0.68	0.58	0.36	0.70	0.43	0.37	0.59
M29	0.86	0.36	0.66	0.52	0.43	0.64	0.59	0.31	0.73	0.46	0.42	0.67
M30	0.27	0.31		0.47	0.46		0.32	0.37		0.43	0.39	
M31							0.43	0.15	0.40	0.55	0.52	0.52
M32							0.65	0.16	0.55	0.53	0.54	0.70
ID	**2013Aut**						**2013Win**					
	SO_4^{2-}	NO_3^-	NH_4^+	EC	OC	TOTAL	SO_4^{2-}	NO_3^-	NH_4^+	EC	OC	TOTAL
M01	0.88	0.59	0.82	0.56	0.76	0.76	0.86	0.57	0.64	0.51	0.46	0.56
M02	0.91	0.58	0.80	0.57	0.76	0.76	0.88	0.56	0.67	0.52	0.50	0.57
M03	0.90	0.59	0.78	0.54	0.76	0.76	0.88	0.58	0.68	0.50	0.47	0.57
M04	0.89	0.58	0.80	0.56	0.77	0.77	0.87	0.55	0.65	0.51	0.49	0.58
M05	0.89	0.58	0.80	0.57	0.79	0.79	0.88	0.57	0.66	0.52	0.49	0.58
M06	0.85	0.58	0.80	0.56	0.73	0.73	0.86	0.56	0.63	0.51	0.49	0.57

Table A3. *Cont.*

ID	2013Aut						2013Win					
	SO_4^{2-}	NO_3^-	NH_4^+	EC	OC	TOTAL	SO_4^{2-}	NO_3^-	NH_4^+	EC	OC	TOTAL
M07	0.88	0.54	0.77	0.57	0.77	0.77	0.90	0.56	0.67	0.52	0.50	0.63
M08	0.88	0.55	0.78	0.57	0.76	0.76	0.88	0.57	0.66	0.52	0.50	0.59
M09	0.88	0.55	0.78	0.57	0.75	0.75	0.87	0.56	0.66	0.52	0.50	0.59
M10												
M11												
M12	0.90	0.54	0.77	0.57	0.77	0.77	0.89	0.57	0.68	0.52	0.50	0.60
M13	0.91	0.57	0.77	0.56	0.77	0.77	0.89	0.55	0.69	0.52	0.47	0.59
M14	0.89	0.55	0.78	0.57	0.73	0.73	0.87	0.58	0.67	0.53	0.50	0.57
M15	0.88	0.56	0.79	0.57	0.76	0.76	0.87	0.58	0.67	0.53	0.50	0.59
M16												
M17												
M18												
M19												
M21	0.88	0.55	0.78	0.57	0.76	0.76	0.52	0.53	0.54	0.52	0.48	0.53
M22	0.88	0.55	0.78	0.57	0.76	0.76	0.87	0.57	0.66	0.52	0.47	0.59
M23	0.88	0.57	0.79	0.56	0.75	0.75	0.87	0.57	0.66	0.51	0.49	0.58
M24	0.88	0.57	0.79	0.56	0.75	0.75	0.87	0.56	0.65	0.51	0.49	0.58
M25	0.91	0.54	0.76	0.58	0.79	0.79	0.87	0.56	0.68	0.52	0.47	0.59
M26	0.89	0.57	0.79	0.56	0.76	0.76	0.87	0.55	0.67	0.51	0.46	0.58
M27	0.91	0.55	0.72	0.72	0.81	0.81	0.88	0.53	0.70	0.62	0.49	0.64
M28	0.92	0.55	0.76	0.58	0.79	0.79	0.88	0.53	0.68	0.51	0.47	0.60
M29	0.92	0.56	0.79	0.58	0.74	0.74	0.91	0.57	0.65	0.54	0.49	0.56
M30	0.20	0.52		0.50			0.46	0.53		0.49	0.46	
M31												
M32												

References

1. World Health Organization. Ambient Air Pollution: A Global Assessment of Exposure and Burden of Disease. Available online: https://www.who.int/phe/publications/air-pollution-global-assessment/en/ (accessed on 14 January 2020).
2. Fiore, A.M.; Naik, V.; Leibensperger, E.M. Air quality and climate connections. *J. Air Waste Manag. Assoc.* **2015**, *65*, 645–685. [CrossRef] [PubMed]
3. Zhang, Q.; Zheng, Y.; Tong, D.; Shao, M.; Wang, S.; Zhang, Y.; Xu, X.; Wang, J.; He, H.; Liu, W.; et al. Drivers of improved PM2.5 air quality in China from 2013 to 2017. *Proc. Natl. Acad. Sci. USA* **2019**, *116*, 24463–24469. [CrossRef] [PubMed]
4. Ministry of the Environment. Available online: http://www.env.go.jp/air/osen/monitoring.html (accessed on 14 January 2020).
5. Chatani, S.; Yamaji, K.; Sakurai, T.; Itahashi, S.; Shimadera, H.; Kitayama, K.; Hayami, H. Overview of Model Inter-Comparison in Japan's Study for Reference Air Quality Modeling (J-STREAM). *Atmosphere* **2018**, *9*, 19. [CrossRef]
6. Carmichael, G.; Sakurai, T.; Streets, D.; Hozumi, Y.; Ueda, H.; Park, S.; Fung, C.; Han, Z.; Kajino, M.; Engardt, M. MICS-Asia II: The model intercomparison study for Asia Phase II methodology and overview of findings. *Atmos. Environ.* **2008**, *42*, 3468–3490. [CrossRef]
7. Carmichael, G.R.; Calori, G.; Hayami, H.; Uno, I.; Cho, S.Y.; Engardt, M.; Kim, S.-B.; Ichikawa, Y.; Ikeda, Y.; Woo, J.H.; et al. model intercomparison of long-range transport and sulfur deposition in East Asia. *Atmos. Environ.* **2002**, *36*, 175–199. [CrossRef]
8. Chen, L.; Gao, Y.; Zhang, M.; Fu, J.-S.; Zhu, J.; Liao, H.; Li, J.; Huang, K.; Ge, B.; Wang, X.; et al. MICS-Asia III: Multi-model comparison and evaluation of aerosol over East Asia. *Atmos. Chem. Phys. Discuss.* **2019**, *2019*, 1–54. [CrossRef]
9. Li, J.; Nagashima, T.; Kong, L.; Ge, B.; Yamaji, K.; Fu, J.-S.; Wang, X.; Fan, Q.; Itahashi, S.; Lee, H.J.; et al. Model evaluation and inter-comparison of surface-level ozone and relevant species in East Asia in the context of MICS-Asia phase III Part I: Overview. *Atmos. Chem. Phys. Discuss.* **2019**, *2019*, 1–56. [CrossRef]

10. Chatani, S.; Morino, Y.; Shimadera, H.; Hayami, H.; Mori, Y.; Sasaki, K.; Kajino, M.; Yokoi, T.; Morikawa, T.; Ohara, T. Multi-Model Analyses of Dominant Factors Influencing Elemental Carbon in Tokyo Metropolitan Area of Japan. *Aerosol Air Qual. Res.* **2014**, *14*, 396–405. [CrossRef]
11. Shimadera, H.; Hayami, H.; Chatani, S.; Morino, Y.; Mori, Y.; Morikawa, T.; Yamaji, K.; Ohara, T. Sensitivity analyses of factors influencing CMAQ performance for fine particulate nitrate. *J. Air Waste Manag. Assoc.* **2017**, *64*, 374–387. [CrossRef]
12. Shimadera, H.; Hayami, H.; Chatani, S.; Morikawa, T.; Morino, Y.; Mori, Y.; Yamaji, K.; Nakatsuka, S.; Ohara, T. Urban Air Quality Model Inter-Comparison Study (UMICS) for Improvement of PM2.5 Simulation in Greater Tokyo Area of Japan. *Asian J. Atmos. Environ.* **2018**, *12*, 139–152. [CrossRef]
13. Chatani, S.; Yamaji, K.; Itahashi, S.; Saito, M.; Takigawa, M.; Morikawa, T.; Kanda, I.; Miya, Y.; Komatsu, H.; Sakurai, T.; et al. Identifying key factors influencing model performance on ground-level ozone over urban areas in Japan through model inter-comparisons. *Atmos. Environ.* **2020**, 223. [CrossRef]
14. Itahashi, S.; Yamaji, K.; Chatani, S.; Hayami, H. Refinement of Modeled Aqueous-Phase Sulfate Production via the Fe- and Mn-Catalyzed Oxidation Pathway. *Atmosphere* **2018**, *9*, 132. [CrossRef]
15. Skamarock, W.C.; Klemp, J.B.; Dudhia, J.; Gill, D.O.; Barker, D.M.; Duda, M.G.; Huang, X.Y.; Wang, W.; Powers, J.G. *A Description of the Advanced Research WRF Version 3*; University Corporation for Atmospheric Research: Boulder, CO, USA, 2008.
16. NCEP FNL Operational Model Global Tropospheric Analyses, continuing from July 1999. *Research Data Archive at the National Center for Atmospheric Research*; Computational and Information Systems Laboratory: Boulder, CO, USA, 2000.
17. Gemmill, W.; Katz, B.; Li, X. Daily Real-Time, Global Sea Surface Temperature a High-Resolution Analysis: RTG_SST_HR, NOAA/NWS/NCEP/EMC/MMAB, Science Application International Corporation, and Joint Center for Satellite Data Assimilation Technical Note Nr. *NOAA/NWS/NCEP/MMAB Off. Note* **2007**, *260*, 1–39.
18. Hong, S.Y.; Dudhia, J.; Chen, S.H. A revised approach to ice microphysical processes for the bulk parameterization of clouds and precipitation. *Mon. Weather Rev.* **2004**, *132*, 103–120. [CrossRef]
19. Mlawer, E.J.; Taubman, S.J.; Brown, P.D.; Iacono, M.J.; Clough, S.A. Radiative transfer for inhomogeneous atmospheres: RRTM, a validated correlated-k model for the longwave. *J. Geophys Res. Atmos* **1997**, *102*, 16663–16682. [CrossRef]
20. Dudhia, J. Numerical Study of Convection Observed during the Winter Monsoon Experiment Using a Mesoscale Two-Dimensional Model. *J. Atmos. Sci.* **1989**, *46*, 3077–3107. [CrossRef]
21. Chen, F.; Dudhia, J. Coupling an advanced land surface-hydrology model with the Penn State-NCAR MM5 modeling system. Part I: Model implementation and sensitivity. *Mon. Weather Rev.* **2001**, *129*, 569–585. [CrossRef]
22. Nakanishi, M.; Niino, H. An improved mellor-yamada level-3 model: Its numerical stability and application to a regional prediction of advection fog. *Bound. Layer Meteorol.* **2006**, *119*, 397–407. [CrossRef]
23. Kain, J.-S. The Kain-Fritsch convective parameterization: An update. *J. Appl. Meteorol.* **2004**, *43*, 170–181. [CrossRef]
24. Byun, D.; Schere, K.L. Review of the Governing Equations, Computational Algorithms, and Other Components of the Models-3 Community Multiscale Air Quality(CMAQ) Modeling System. *Appl. Mech. Rev.* **2006**, *59*, 51–77. [CrossRef]
25. Ramboll Environment and Health. User's Guide Comprehensive Air Quality Model with Extensions. Available online: http://www.camx.com/files/camxusersguide_v6-50.pdf (accessed on 14 January 2020).
26. Grell, G.A.; Peckham, S.E.; Schmitz, R.; McKeen, S.A.; Frost, G.; Skamarock, W.C.; Eder, B. Fully coupled "online" chemistry within the WRF model. *Atmos. Environ.* **2005**, *39*, 6957–6975. [CrossRef]
27. Carter, W.P.L. Documentation of the SAPRC-99 chemical mechanism for VOC reactivity assessment. *Contract* **2000**, *92*, 95–308.
28. Carter, W.P.L. Development of the SAPRC-07 chemical mechanism. *Atmos. Environ.* **2010**, *44*, 5324–5335. [CrossRef]
29. Whitten, G.Z.; Heo, G.; Kimura, Y.; McDonald-Buller, E.; Allen, D.T.; Carter, W.P.L.; Yarwood, G. A new condensed toluene mechanism for Carbon Bond CB05-TU. *Atmos. Environ.* **2010**, *44*, 5346–5355. [CrossRef]
30. Goliff, W.S.; Stockwell, W.R.; Lawson, C.V. The regional atmospheric chemistry mechanism, version 2. *Atmos. Environ.* **2013**, *68*, 174–185. [CrossRef]

31. Binkowski, F.S. Models-3 Community Multiscale Air Quality (CMAQ) model aerosol component 1. Model description. *J. Geophys. Res.* **2003**, 108. [CrossRef]
32. Koo, B.; Knipping, E.; Yarwood, G. 1.5-Dimensional volatility basis set approach for modeling organic aerosol in CAMx and CMAQ. *Atmos. Environ.* **2014**, *95*, 158–164. [CrossRef]
33. Nenes, A.; Pandis, S.N.; Pilinis, C. ISORROPIA: A new thermodynamic equilibrium model for multiphase multicomponent inorganic aerosols. *Aquat. Geochem.* **1998**, *4*, 123–152. [CrossRef]
34. Nenes, A.; Pandis, S.N.; Pilinis, C. Continued development and testing of a new thermodynamic aerosol module for urban and regional air quality models. *Atmos. Environ.* **1999**, *33*, 1553–1560. [CrossRef]
35. Fountoukis, C.; Nenes, A. ISORROPIA II: A computationally efficient thermodynamic equilibrium model for K^+-Ca^{2+}-Mg^{2+}-$Nh_4{}^+$-Na^+-$SO_4{}^{2-}$-$NO_3{}^-$-Cl^--H_2O aerosols. *Atmos. Chem. Phys.* **2007**, *7*, 4639–4659. [CrossRef]
36. Carlton, A.G.; Bhave, P.V.; Napelenok, S.L.; Edney, E.D.; Sarwar, G.; Pinder, R.W.; Pouliot, G.A.; Houyoux, M. Model Representation of Secondary Organic Aerosol in CMAQv4.7. *Environ. Sci. Technol.* **2010**, *44*, 8553–8560. [CrossRef]
37. Itahashi, S.; Yamaji, K.; Chatani, S.; Hisatsune, K.; Saito, S.; Hayami, H. Model Performance Differences in Sulfate Aerosol in Winter over Japan Based on Regional Chemical Transport Models of CMAQ and CAMx. *Atmosphere* **2018**, *9*, 488. [CrossRef]
38. Ackermann, I.J.; Hass, H.; Memmesheimer, M.; Ebel, A.; Binkowski, F.S.; Shankar, U. Modal aerosol dynamics model for Europe: Development and first applications. *Atmos. Environ.* **1998**, *32*, 2981–2999. [CrossRef]
39. Schell, B.; Ackermann, I.J.; Hass, H.; Binkowski, F.S.; Ebel, A. Modeling the formation of secondary organic aerosol within a comprehensive air quality model system. *J. Geophys. Res. Atmos* **2001**, *106*, 28275–28293. [CrossRef]
40. Sudo, K.; Takahashi, M.; Kurokawa, J.; Akimoto, H. CHASER: A global chemical model of the troposphere - 1. Model description. *J. Geophys. Res. Atmos.* **2002**, 107. [CrossRef]
41. Huang, M.; Carmichael, G.R.; Pierce, R.B.; Jo, D.S.; Park, R.J.; Flemming, J.; Emmons, L.K.; Bowman, K.W.; Henze, D.K.; Davila, Y.; et al. Impact of intercontinental pollution transport on North American ozone air pollution: An HTAP phase 2 multi-model study. *Atmos. Chem. Phys.* **2017**, *17*, 5721–5750. [CrossRef] [PubMed]
42. Janssens-Maenhout, G.; Crippa, M.; Guizzardi, D.; Dentener, F.; Muntean, M.; Pouliot, G.; Keating, T.; Zhang, Q.; Kurokawa, J.; Wankmuller, R.; et al. HTAP_v2.2: A mosaic of regional and global emission grid maps for 2008 and 2010 to study hemispheric transport of air pollution. *Atmos. Chem. Phys.* **2015**, *15*, 11411–11432. [CrossRef]
43. van der Werf, G.R.; Randerson, J.T.; Giglio, L.; van Leeuwen, T.T.; Chen, Y.; Rogers, B.M.; Mu, M.; van Marle, M.J.E.; Morton, D.C.; Collatz, G.J.; et al. Global fire emissions estimates during 1997–2015. *Earth Syst. Sci. Data Discuss.* **2017**, *2017*, 1–43. [CrossRef]
44. Chatani, S.; Morikawa, T.; Nakatsuka, S.; Matsunaga, S.; Minoura, H. Development of a framework for a high-resolution, three-dimensional regional air quality simulation and its application to predicting future air quality over Japan. *Atmos. Environ.* **2011**, *45*, 1383–1393. [CrossRef]
45. Diehl, T.; Heil, A.; Chin, M.; Pan, X.; Streets, D.; Schultz, M.; Kinne, S. Anthropogenic, biomass burning, and volcanic emissions of black carbon, organic carbon, and SO_2 from 1980 to 2010 for hindcast model experiments. *Atmos. Chem. Phys. Discuss.* **2012**, *2012*, 24895–24954. [CrossRef]
46. Japan Meteorological Agency. Available online: http://www.data.jma.go.jp/svd/vois/data/tokyo/volcano.html (accessed on 14 January 2020).
47. Guenther, A.B.; Jiang, X.; Heald, C.L.; Sakulyanontvittaya, T.; Duhl, T.; Emmons, L.K.; Wang, X. The Model of Emissions of Gases and Aerosols from Nature version 2.1 (MEGAN2.1): An extended and updated framework for modeling biogenic emissions. *Geosci. Model Dev.* **2012**, *5*, 1471–1492. [CrossRef]
48. Tetsuo Fukui, K.K. Tsuyoshi Baba, Akiyoshi Kannari. Updating EAGrid2000-Japan emissions inventory based on the recent emission trends. *J. Jpn. Soc. Atmos. Environ.* **2014**, *49*, 9.
49. Kannari, A.; Tonooka, Y.; Baba, T.; Murano, K. Development of multiple-species 1km×1km resolution hourly basis emissions inventory for Japan. *Atmos. Environ.* **2007**, *41*, 3428–3439. [CrossRef]
50. Zhang, Q.; Streets, D.G.; Carmichael, G.R.; He, K.B.; Huo, H.; Kannari, A.; Klimont, Z.; Park, I.S.; Reddy, S.; Fu, J.-S.; et al. Asian emissions in 2006 for the NASA INTEX-B mission. *Atmos. Chem. Phys.* **2009**, *9*, 5131–5153. [CrossRef]

51. Emmons, L.K.; Walters, S.; Hess, P.G.; Lamarque, J.F.; Pfister, G.G.; Fillmore, D.; Granier, C.; Guenther, A.; Kinnison, D.; Laepple, T.; et al. Description and evaluation of the Model for Ozone and Related chemical Tracers, version 4 (MOZART-4). *Geosci. Model Dev.* **2010**, *3*, 43–67. [CrossRef]
52. Emery, C.; Liu, Z.; Russell, A.G.; Odman, M.T.; Yarwood, G.; Kumar, N. Recommendations on statistics and benchmarks to assess photochemical model performance. *J. Air Waste Manag. Assoc.* **2017**, *67*, 582–598. [CrossRef] [PubMed]
53. Boylan, J.W.; Russell, A.G. PM and light extinction model performance metrics, goals, and criteria for three-dimensional air quality models. *Atmos. Environ.* **2006**, *40*, 4946–4959. [CrossRef]
54. Zhang, Y.; He, J.; Zhu, S.; Gantt, B. Sensitivity of simulated chemical concentrations and aerosol-meteorology interactions to aerosol treatments and biogenic organic emissions in WRF/Chem. *J. Geophys. Res. Atmos.* **2016**, *121*, 6014–6048. [CrossRef]
55. Alexander, B.; Park, R.J.; Jacob, D.J.; Gong, S. Transition metal-catalyzed oxidation of atmospheric sulfur: Global implications for the sulfur budget. *J. Geophys. Res.* **2009**, 114. [CrossRef]
56. Jacobson, M.Z. Development and application of a new air pollution modeling system.2. Aerosol module structure and design. *Atmos. Environ.* **1997**, *31*, 131–144. [CrossRef]
57. Martin, L.R.; Good, T.W. Catalyzed Oxidation of Sulfur-Dioxide in Solution-The Iron-Manganese Synergism. *Atmos. Environ. Part A Gen. Top.* **1991**, *25*, 2395–2399. [CrossRef]
58. Siefert, R.L.; Johansen, A.M.; Hoffmann, M.R.; Pehkonen, S.O. Measurements of trace metal (Fe, Cu, Mn, Cr) oxidation states in fog and stratus clouds. *J. Air Waste Manag. Assoc.* **1998**, *48*, 128–143. [CrossRef] [PubMed]